A FINITE ELEMENT STUDY ON THE MEDIAL PATELLOFEMORAL LIGAMENT RECONSTRUCTION

A Thesis

Presented to

The Graduate Faculty of The University of Akron

In Partial Fulfillment

of the Requirements for the Degree

Master of Science

Bharath Koya

December, 2013

A FINITE ELEMENT STUDY ON THE MEDIAL PATELLOFEMORAL LIGAMENT RECONSTRUCTION

Bharath Koya

Thesis

Approved:

_____	_____
Co-Advisor Dr. Marnie Saunders	Department Chair Dr. Brian L. Davis
_____	_____
Co-Advisor Dr. John Elias	Dean of the College Dr. George Haritos
_____	_____
Committee Member Dr. Mary C. Verstraete	Dean of the Graduate School Dr. George R. Newkome
	_____
	Date

ABSTRACT

Patellar instability is a major problem among young individuals. Chronic patellar instability termed as patellar dislocation occurs mainly due to the reduction in the medial restraining forces for the patella, excessive Q-angle, patella alta and trochlear dysplasia. It causes a tear of the medial patellofemoral ligament (MPFL) in the majority of instances. The MPFL is the main passive stabilizer preventing patellar instability and accounts for 50-60 % of the total restraining forces. Reconstruction of the torn MPFL is a surgical option performed in chronic cases to improve patellofemoral biomechanics and to provide better stability at the knee. Finite element analysis (FEA) makes it possible to simulate the surgical technique of reconstruction of the MPFL, observe the effects on the articular cartilage structures and determine the patellofemoral kinematics, which is not possible with in vivo imaging analysis. In the present study, subject specific computational (finite element) models were built in ABAQUS based on the 3D anatomical geometry of the patellofemoral joint from pre–op MRI scans. The femur and patella were modeled as rigid structures with quadrilateral elements. Patellofemoral articular cartilage was modeled as isotropic elastic structures with hexahedral elements. The quadriceps muscle group, patellar tendon and the MPFL graft were represented using linear tension-only springs. The quadriceps muscle force was calculated from the foot load that

the patient was able to withstand at a particular flexion angle during the MRI scan. The MPFL reconstruction surgery was simulated by modeling the ligament with uniaxial connector elements and material properties representing the graft material. FE simulations with appropriate boundary and loading conditions showed that the lateral translation was restricted with a MPFL graft. Validation of these FE models was done by comparing the results with the kinematics obtained from an analysis based on MRI scans taken before and after the MPFL reconstruction surgery. FEA results matched the trends observed in the results of the experimental study, but they failed to replicate them quantitatively. In addition, the ratio of tension in the patellar tendon and quadriceps muscles and the tension in the MPFL graft elements was obtained from the simulations. The technique used in the present study can be improved by dealing with the limitations of the modeling like meshing of the structures and material properties. The FE models can be used to study the inter-subject differences, graft attachment points and graft tensioning to help with the ligament reconstruction procedures.

ACKNOWLEDGEMENTS

I would like to take this opportunity to thank all those people who have helped me directly or indirectly throughout my Masters.

First and foremost, I would like to express my sincere and heartfelt gratitude to Dr. John Elias for supervising me. It would have been impossible for me to learn so many new things in the field of Computational Biomechanics without the constant guidance and help from him. I would also like to thank Dr. Marnie Saunders and Dr. Mary C Verstraete for advising me all through my Masters.

I would like to thank Archana Saranathan and Kushal Shah for taking their time and having discussions with me. Both of them have helped me develop the subject specific finite element models. I would also like to thank the faculty and staff of the Department of Biomedical Engineering, The University of Akron.

I would like to thank my family and friends for giving me the support and encouragement at every stage. The National Institute of Arthritis and Musculoskeletal and Skin Disorders, Award Number R03AR054910 provided financial support for the project.

TABLE OF CONTENTS

Page

LIST OF FIGURES

Figure Page

CHAPTER I

INTRODUCTION

Computational studies based on finite element modeling (FEM) for which validation is performed either by in vitro or experimental imaging analysis are gaining increased recognition in the field of biomechanics. In recent years, many studies were performed using subject specific FE models. For an orthopedic surgeon dealing with a clinical problem or an injury of a particular joint, these subject specific FE models offer the advantage of studying a number of factors computationally. The surgeon can then come to a conclusion based on these studies which help in determining what factors (for example: ligament attachment points, graft tensioning, patella position) contribute to the success of the procedure being followed [60, 61, 64].

In the present study, the computational modeling technique has been applied to study patellar instability. Patellar instability is a malalignment of the patella restricting the motion at the knee joint and thereby affecting daily activities. A serious form of patellar instability such as patellar dislocation, may result from anatomical conditions such as reduction in the medial restraining forces for the patella, patella alta, excessive Q-angle and trochlear dysplasia [31]. Dislocation is seen in situations involving sudden and large forces acting on the knee in the

lateral direction or a twisting motion. The average number of clinical cases involving the patellar dislocation among young adult population was reported to be 5.8 males and 7 females per 100,000 persons [6]. The same problem was found to occur within the age group from 10-17 years with an average of 29 per 100,000 persons per year [6]. In most instances, an individual experiences a small tear or rupture to the MPFL during dislocation [48, 49].

1.1 Medial patellofemoral ligament

The MPFL is a thin, fan shaped retinacular structure. It connects the patella and femur on the medial side and is the main static stabilizer of the patella against excessive lateral shift. The observation that the MPFL prevents maltracking of the patella out of the trochlea groove in the first 30° of knee flexion has been confirmed by many in vitro studies [21, 22, 26, 44, 58]. This ligament is commonly involved in patellar instability and is either torn or damaged depending on the severity of the injury.

Reconstruction of this ligament is performed to restore stability. This helps in restoring the normal anatomy and kinematics and prevents the articular cartilage from being further damaged. Reconstruction is usually performed with graft materials taken from the subject's own body or artificial materials. Gomes et al. (2004) used a semitendinosus autograft, Siebold et al. (2010) used a hamstrings graft and Nomura et al. (2000) performed the reconstruction surgeries with a Leeds–Keio artificial ligament. Although the graft materials were different, the reconstruction of the ligament caused a reduction in the recurrence rates and in the lateral subluxation and tilt of patella. In vitro studies were also performed

based on cadaver specimens addressing patellofemoral kinematics with the MPFL reconstruction [54, 85]. These studies reported that an anatomical reconstruction of the damaged ligament improved the stability of the patella. Small changes in the graft fixation during reconstruction may increase the patellofemoral pressures and tension in the graft in flexion, as demonstrated by the computational models in Elias and Cosgarea's study [63]. These errors might also result in articular cartilage degradation, patellofemoral pain and arthrosis of the knee joint as reported by Parikh et al. (2013). To avoid such complications, computational studies help by studying the various factors associated with the surgery.

Computational models based on FEM have been built to study the patellofemoral joint contact areas [42], joint stresses [67, 82] and biomechanics of the joint under various loading conditions [51, 68]. Previous studies were also based on modeling of the anterior cruciate and medial collateral ligaments [81, 83]. However, there are no previous FEA studies based on the influence of the MPFL reconstruction exclusively on the in vivo kinematics of a symptomatic knee.

1.2 Objectives

The objectives of the present computational study were:

(a) To develop a computational finite element model for the symptomatic knee with subject specific anatomical geometry.

(b) To study the kinematics of the patellofemoral joint before and after the ligament reconstruction surgery and to validate the finite element models with these parameters.

(c) To compute the tensions in the patella tendon, quadriceps muscles and the MPFL graft using the finite element models.

1.3 Statement of hypothesis

Null hypothesis: The kinematics of the patellofemoral joint FEA model developed from a symptomatic knee (computed with pre-op and post-op MRI data) can be validated with those from MRI image analysis.

$$H_0: \mu_{FEA} = \mu_{(image\ analysis)}$$

Alternate hypothesis: The kinematics of the patellofemoral joint FEA model developed from a symptomatic knee cannot be validated by comparing with those from MRI image analysis.

$$H_a: \mu_{FEA} \neq \mu_{(image\ analysis)}$$

CHAPTER II

BACKGROUND

2.1 Anatomy of patellofemoral joint

Any movement related activity we perform in our daily life involves the lower extremities of which the knee is an indispensable part. It is a synovial type of hinge joint and is comprised of two components; the patellofemoral joint and the tibiofemoral joint. The patellofemoral joint is a saddle shaped joint formed by the articulation of the distal femur with the patella, while the tibiofemoral joint is formed by the articulation of the distal femur and the proximal tibia [1]. The knee bears the entire body weight with the help of these two components.

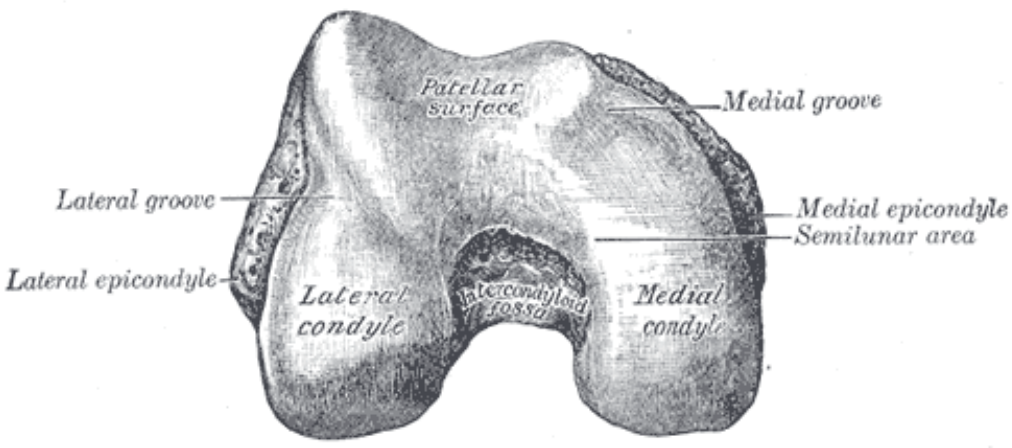

Figure 2.1: Condyles of the distal femur.

Courtesy: Gray, Henry. Anatomy of the Human Body. Bartleby.com. [1]

The distal femur is cuboidal shaped with two condyles one on each of the medial and lateral sides [1]. These two condyles (Figure 2.1) are divided by the trochlear groove (i.e. patellar surface depression) between them, which helps in the stability of the patella. The lateral condyle is usually at a slightly elevated height and slope when compared to the medial condyle [3]. On the sides of both the condyles, slight convex prominences called epicondyles are found. The triangular bone patella is the main component of the knee joint serving as a fulcrum. The superior border of the patella is a flat surface, while the inferior border is more like an apex and the anterior surface is a bit convex (Figure 2.2). The posterior surface has a medial and lateral facet separated by a ridge. Fluid chambers called bursae cover the anterior surface of the patella below the skin and reduces friction [3].

Figure 2.2: Anterior surface of the patella (on the left) and posterior surface of the patella (on the right).

Courtesy: Gray, Henry. Anatomy of the Human Body. Bartleby.com. [1]

Muscles and ligaments surround the knee joint. The quadriceps muscles which are important in the thigh region are asymmetric and formed by the muscle bands rectus femoris, vastus intermedius (VI), vastus lateralis (VL) and vastus medialis (VM) (Figure 2.3) [3]. The insertions of the quadriceps muscles are on the supero-proximal border of the patella. The rectus femoris, which originates from the anterior inferior iliac spine of pelvis, is the most anterior muscle band inserting onto the superior border of the patella. It is continuous distally with the fibers of the patella tendon. Below this, the VI originates from the anterior and lateral femoral shaft and inserts onto the superior aspect of the patella. The VM muscle band originates from the linea aspera and intertrochanteric line of the femur and inserts onto the superior medial patella border. The distal fibers of this muscle band form the vastus medialis obliqus (VMO) component, which supports the patella medially. Similar to the VM, but less acute and inserting onto the superior lateral border of the patella is the VL. The VL muscle band originates at the linea aspera and greater trochanter of the femur. Originating at the distal and inferior patella border and inserting onto the tibial tubercle is the patella tendon (Figure 2.3). The loads generated by the contraction of the quadriceps group are transmitted to the lower extremity through patella tendon muscle fibers.

Just like every other bone in the human body is covered by a soft tissue layer at a joint, the patella also has articular cartilage. This cartilage, with a thickness of about 5 mm, covers the posterior surface of the patella and interacts with the femoral articular cartilage [2, 4]. The patella experiences high compressive loads with minimal structural damage in normal activities, with the thick cartilage layer

offering the necessary protection and load distribution capabilities. The femoral articular cartilage covers the trochlear groove and distal condyles. The cartilage corresponding to the posterior surface interacts with the menisci on the tibial surface. The synovial fluid between the two interacting articular surfaces (i.e. on the patella and on the femur) reduces the frictional force between them.

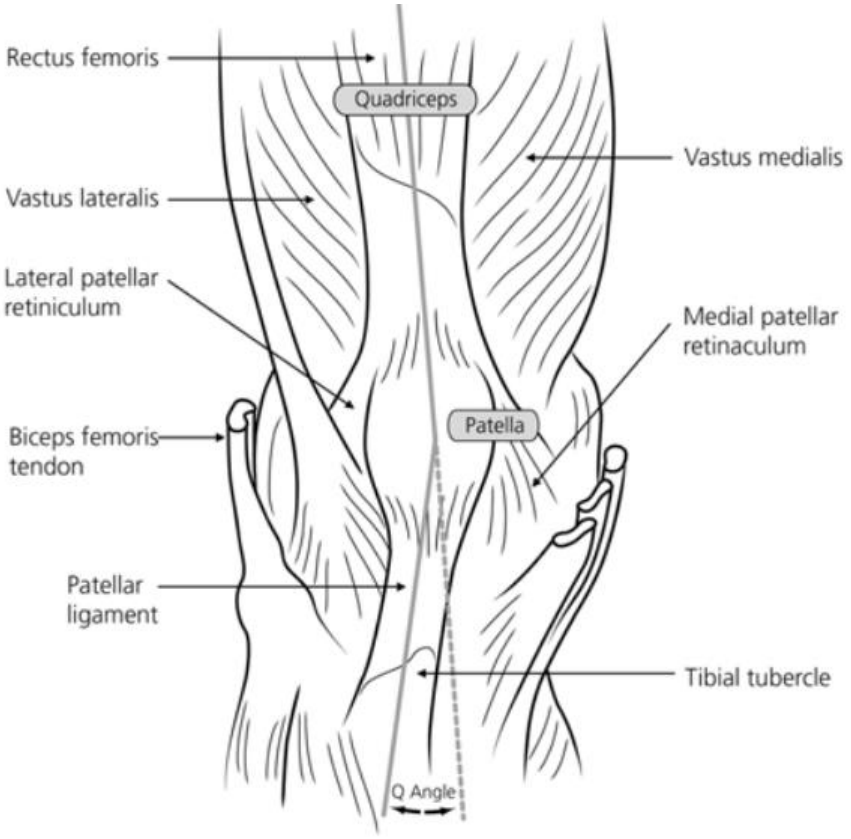

Figure 2.3: Anatomy of the patellofemoral joint with the surrounding muscles and ligamentous structures.

Used with permission from Dath, R., Chakravarthy, J., & Porter, K. (2006). Patella dislocations. *Trauma*, *8*(1), 5–11. [13]

Apart from the muscles, other major components in the patellofemoral joint are the ligaments. These soft tissues connect two bones and aid in transmitting the forces and restricting the motion of the patella. There are two primary

patellofemoral ligaments i.e. medial patellofemoral ligament and lateral patellofemoral ligament [22]. Other prominent ligaments in the knee connecting the femur and tibia are the anterior and posterior cruciate ligaments and the medial and lateral collateral ligaments.

2.2 Stability of the patella

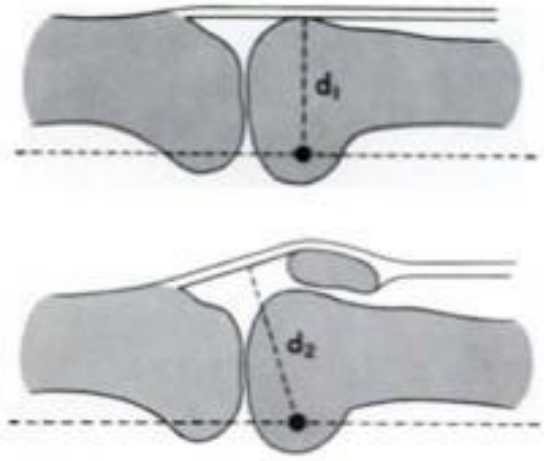

Figure 2.4: Moment arm of the quadriceps (d2>d1).

Used with permission from Kaufer H., Mechanical function of the Patella. 1971, *J Bone Joint Surg Am.* Dec 01; 53 (8): 1551-1560. [9]

The patella is a key component of the knee joint. The stability of this sesamoid structure is important at all flexion angles of the knee, which is influenced and controlled by the bony geometry, the quadriceps muscles and the passive soft tissue ligaments surrounding it [23]. The most important function of the patella is to act as a fulcrum for the muscular contraction [3]. In addition, it also protects the distal femur and its condyles. It increases the moment arm of the quadriceps force about the center of rotation of the knee joint (Figure 2.4). The extensor force about the knee, generated by the contraction of the muscles is thus

increased with this mechanism. The quadriceps muscles which control the knee extension mechanism are aided by the patella at all knee positions.

The position of the patella varies as the knee flexes. Starting at full extension and ranging to mid flexion angles, i.e. about 30°-45°, the distal patella interacts with the area proximal to the trochlea and the femoral condyles [7]. The patella does not engage with the trochlear groove until the mid-flexion angles and so it has a free medial-lateral translational degree of freedom. With the major quadriceps muscle orientation in the proximal and lateral direction, the force generated by the contraction of these muscles tries to pull the patella in those directions. The VMO resists the lateral translation by giving an active medial force. While the action of the VMO balances the patella to some degree, the MPFL is found to be the most prominent passive stabilizer of the patella at early knee flexion angles offering about 50–60 % of the restraint force [21, 22, 26]. The muscular contractions of the quadriceps muscles and passive action of the soft tissue ligaments on the medial side thus provide the stability at these early flexion angles.

Once the patella engages within the trochlear groove, the bony geometry of the two condyles controls the stability and allows it to rest and slide within the groove. The lateral condyle of the femur being at a higher elevation and slope compared to the medial condyle, restricts the lateral translation of the patella at these flexion angles [9]. The lack of this bony geometry for support risks the stability at early flexion angles in some cases. Any weakening in the muscle

contributions usually results in maltracking of the patella, i.e. it moves out of the normal path of its motion. Most often, an individual experiencing a twisting motion or a sudden large force has subluxation or a dislocation of the patella at 20°-30° flexion [7, 10].

2.3 Anatomy of the medial patellofemoral ligament

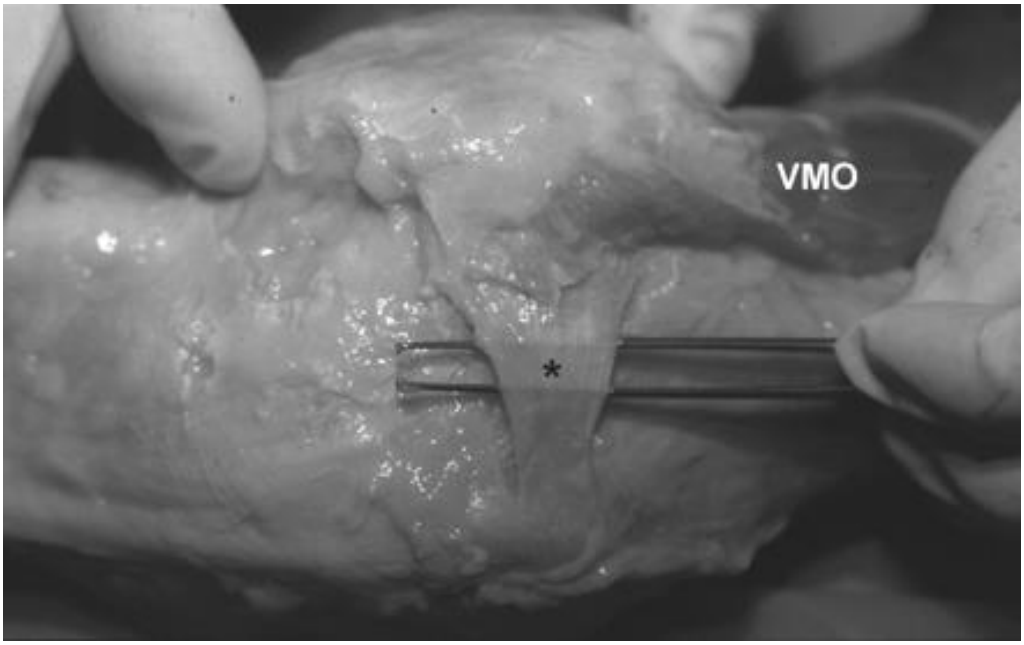

Figure 2.5: Anatomy of the MPFL.

Used with permission from Amis AA, Firer P, Mountney J, Senavongse W, Thomas NP. Anatomy and biomechanics of the medial patellofemoral ligament. *The knee*. 2003; *10*(3): 215–20. [10]

There was a much speculated controversy regarding the existence of the MPFL in the past due to its thin structure. In the recent years, many studies were done to identify this ligament by dissecting fresh cadaver knee specimens [10, 11, 12, 17, 23]. The MPFL, as the name indicates is a ligamentous tissue with its insertions on the superior medial border of the patella and near the adductor tubercle on the medial femoral condyle (Figure 2.5). The MPFL serves as the

primary static soft tissue restraint providing 50-60 % of the restraint forces for the patella to avoid any lateral translation [21, 22, 26]. The contribution of other patellar stabilizing components is minimal in the first 30° of knee flexion [22].

The MPFL is identified in the second of the three layers of medial retinacular structures beside medial collateral ligament, below medial retinaculum and above medial patellomeniscal and medial patellotibial ligaments as described by Warren and Marshall (1979). Many authors have described the presence of this ligament by palpation of the medial side of the knee. Though the rates were low, some authors reported that they failed to detect the presence of the ligament contradicting other studies. While Conlan et al. (1993) was able to detect the ligament in 88 % of the knees (29 out of 33), Reider et al. (1981) could identify it only in 35 % of the knees (7 out of 20).

The MPFL is an oblique retinacular structure. It has insertions on the femoral medial condyle near the adductor tubercle and the proximal half on the superior medial border of the patella. The MPFL insertion on the femoral side is proximal and posterior to the medial epicondyle and anterior and distal to the adductor tubercle (Figures 2.6, 2.7) [14]. The measurements of the femoral insertion with respect to other structures varied with different dissection studies and controversy still exists as to where exactly the insertion location was found. Inferior straight bundle and superior oblique bundle are the two functional bundles of the MPFL forming the shape and contributing to the size of the ligament.

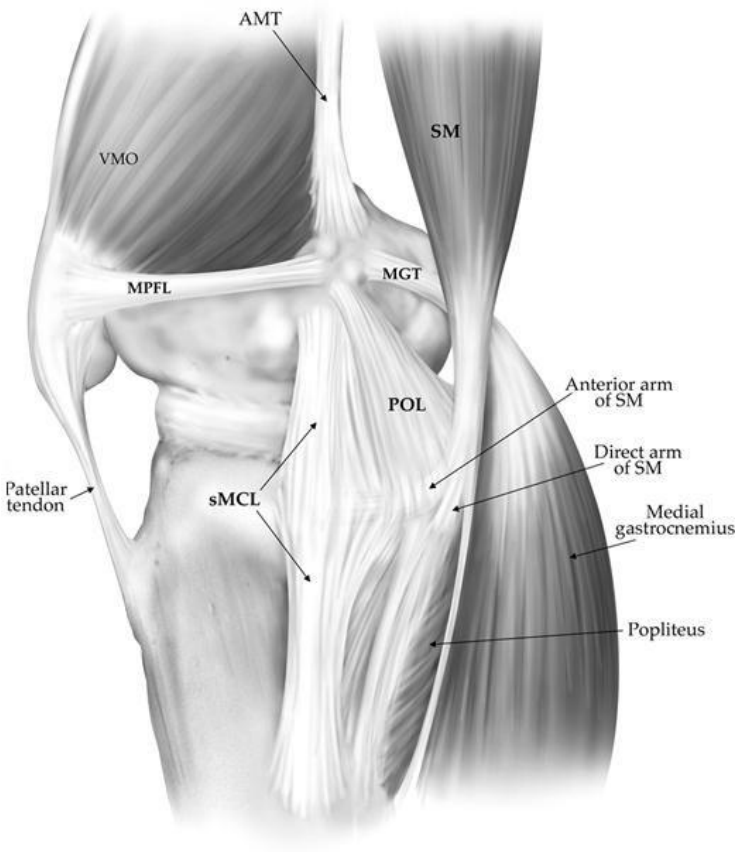

Figure 2.6: Anatomy of the knee on the medial side.

Used with permission from LaPrade RF, Engebretsen AH, Ly TV, Johansen S, Wentorf FA, Engebretsen L. The anatomy of the medial part of the knee. J Bone Joint Surg Am. 2007 Sep; 89(9): 2000-10. [14]

The length of the ligament is 58 mm ranging from 47 – 70 mm [12]. The width of the ligament varies between 3 – 30 mm over the complete length of the ligament [10]. At the midpoint, thickness of the MPFL was observed to be 0.44 ± 0.19 mm and width to be 12 ± 3 mm by Nomura et al. (2000). Being a fan shaped structure, the MPFL is wider at the patellar end when compared to the femoral side. The tension in the ligament varies with the change in the position of the patella. It is tight in the lower flexion angles offering the required resistance to lateral translation of patella and slack at higher flexion angles.

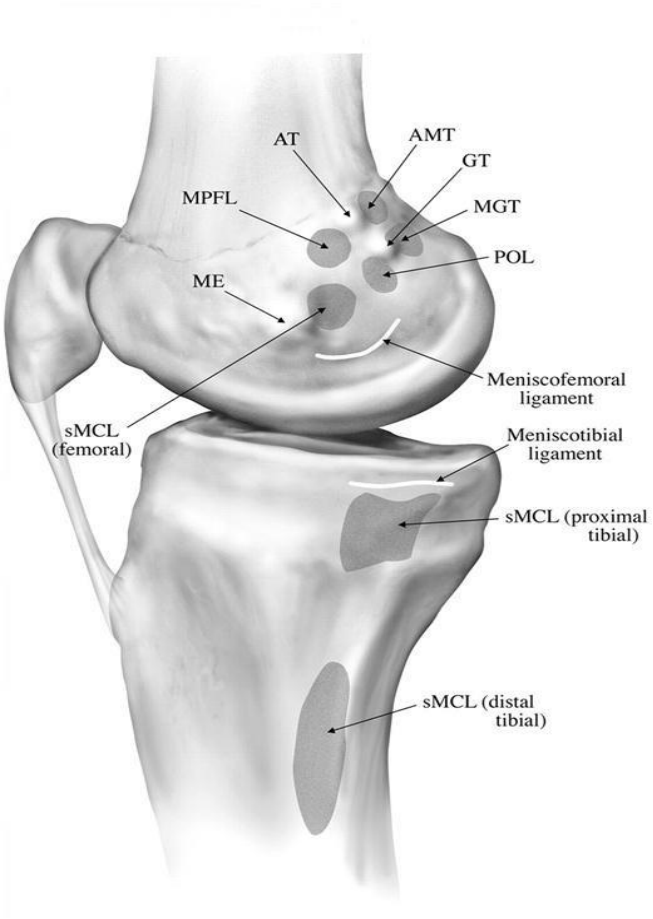

Figure 2.7: Femoral attachment location of the MPFL with respect to other structures.

Used with permission from LaPrade RF, Engebretsen AH, Ly TV, Johansen S, Wentorf FA, Engebretsen L. The anatomy of the medial part of the knee. J Bone Joint Surg Am. 2007 Sep; 89(9): 2000-10. [14]

The strength of the native MPFL was determined by biomechanical tests. Tensile tests were conducted on 10 cadaveric specimens by Amis et al. (2003). In their experiment, the patella was pulled away from the femur in the anterolateral direction. The MPFL served as the only link connecting the patella with the femur. They report that the mean failure load was 208 N [10]. When compared to other knee ligaments like the ACL (anterior cruciate ligament) and the PCL (posterior cruciate ligament), this is relatively small. Nevertheless, the native and

intact MPFL serves as the major restraint against the lateral translation of the patella before it enters the trochlear groove. Biomechanical tests were conducted to determine the percentage of lateral restraining force offered by the MPFL which was observed to be 50-60 % [21, 22, 26]. The MPFL also serves as a supporting structure for the patella in having a smooth entry into the trochlear groove [10]. Any rupture or tear of this ligament reduces the passive restraining force resisting the lateral tilt and translation of the patella.

Nomura et al. (1999) studied the injuries associated with the MPFL and identified two types. The first type is an avulsion type of injury, which is a tear usually at the femoral insertion and the second is a substantial type of injury, a complete rupture or tear of the ligament. The femoral insertion which is thinner than the patellar insertion is usually found to be the site of detachment (Figure 2.6) [89]. It was observed by Sallay et al. (1996) through surgical examinations that 94 % of the patients with acute patellar dislocations present themselves with a MPFL tear. Many techniques have been described in the literature for the reconstruction of the MPFL with different graft materials. Hamstrings graft, gracilis tendon autograft, semitendinosus tendon autograft, polyester ligament and Leeds-Keio artificial ligament are the different types of graft materials available for the reconstruction of the MPFL. All these procedures are targeted towards the same goal i.e. to restore the normal anatomy of the joint and with an aim to reduce the lateral translation of the patella.

The reconstruction of the ligament is planned after considering a number of factors so that the individual does not experience complications after undergoing

the surgical procedure. These complications arise due to either the technical issues or the anatomical choices and are mostly pronounced in young patients leading to recurrent dislocations. Parikh et al. (2013) observed that about 16.2 % of the knees out of 179 knees which underwent MPFL reconstruction resulted in post-op problems. The young pediatric patients have their growth plates still open at the distal femoral physis and so the choice of the femoral attachment points for the ligament graft is of utmost importance. Having the femoral tunnel positioned in the epiphysis avoids damaging and preventing injury to the growth plate [88]. Schottle et al. (2007), Servien et al. (2011), Stephen et al. (2012), Yoo et al. (2012) examined the effects of malpositioning the graft on the femoral side and found that it results in non-physiological loading conditions. Proximal positioning of the ligament on the femoral side would lead to elongation as the knee flexes and slackens the ligament as the knee extends. The distal positioning reversed the effects of the proximal positioning. Malpositioning of the ligament in this way does not provide enough tension to the ligament in knee flexion and extension. Schottle et al. (2007) provided a 5 mm diameter for the MPFL insertion on the femoral side based on their study and the descriptions provided by Smirk and Morris (2003). Thaunat et al. (2008) recommends patella drill holes with minimum diameter to avoid fracture of the patella. Elias and Cosgarea (2006) studied the complications of the MPFL reconstructions with the help of the computational models. The graft, when proximally malpositioned on the femoral side and with a short resting length compared to the intact MPFL, resulted in the medial articular cartilage surface having excessive forces and pressures. Overtensioning of the

graft might also affect the medial cartilage pressures [59]. These errors might result in articular cartilage related problems, arthritis and pain at the knee joint. A surgeon needs to take care of all these issues while performing a MPFL reconstruction surgery.

2.4 Patellar instability

Malalignment of the patella out of its normal path leads to pain and discomfort. In addition, the individual also experiences cartilage degradation problems. This usually leads to stability problems of the patella and occurs most often at knee flexion angles between 20° and 30° [7, 10].

2.4.1 Patellar subluxation

Patellar subluxation is an acute case of patellar instability and usually involves a partial movement of the patella out of its normal path along the trochlear groove. A weakening of the quadriceps muscles or large force acting on the knee in the lateral direction results in the patella being partially displaced out of the trochlea. In such cases, the patella is neither stabilized by the trochlear groove of the femoral condyles nor by the quadriceps muscles and this leads to discomfort, intense pain and swelling at the joint. Non-operative treatment is followed commonly for treating this disorder after diagnosing the affected knee either with an x-ray, CT or MRI.

2.4.2 Patella dislocation

Figure 2.8: Lateral patella dislocation at the time of surgery.

Used with permission from Noyes FR, Albright JC. Reconstruction of the medial patellofemoral ligament with autologous quadriceps tendon. *Art hroscopy*. 2006; 22: 904.e1 – 904.e7. [15]

The patella dislocates from the normal position either when an excessive quadriceps contraction occurs or when a large force acts in the lateral direction. Bony abnormalities such as a flat trochlea i.e. trochlear dysplasia, patella alta, muscle weakness, or a ligament deficiency are some of the factors resulting in dislocation (Figure 2.8). After the initial dislocation of the patella from the trochlear groove, an MRI or x-ray of the affected knee provides radiographical evidence of the tear or rupture of the MPFL (Figure 2.9) [30].

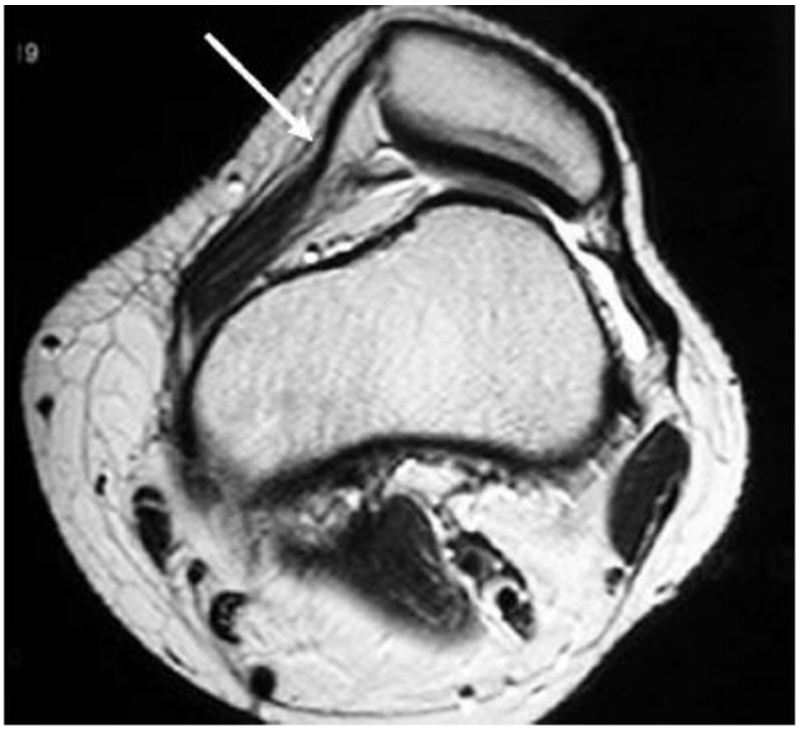

Figure 2.9: Axial MR demonstrating a stretched MPFL associated with patella dislocation out of the trochlear groove in case of patella alta.

Used with permission from Neil Upadhyay, Charles Wakeley, Jonathan D.J. Eldridge. Patellofemoral instability. Orthopaedics and Trauma. 2010, April; 24(2): 139 – 148. [30]

Though the patella dislocation mainly involves the patellar tracking, another problem is with the articular cartilage beneath it. The cartilage degrades and erodes over long periods of time causing chondromalacia and discomfort. This affects the synovial joint and thus the ability of the knee joint to perform natural activities and function normally. Immediate treatment is provided with the non-operative methods and after a careful examination, an operative procedure is followed to treat the malaligment.

2.5 Treatment options for patellar instability

2.5.1 Non-operative methods

Conservative methods like bracing and physical therapy which involve muscle strengthening exercises are the most common non-operative options to treat patellar instability. For immediate pain relief to the individuals suffering with patella instability, many surgeons recommend the use of bracing which offers the advantage of restricting the lateral displacement. Powers et al. (2004) observed an increase in the patellofemoral contact area when bracing was used. In addition, the increase in contact area reduced the average joint stress and the patellofemoral pain [29]. The patella subluxation problem is usually treated with muscle strengthening exercises involving the quadriceps and hamstring muscles of the lower extremity to avoid having an operative procedure and preserve the natural tissues.

In a study conducted to determine the effectiveness of conservative treatment procedures by Cofield and Bryan (1977), out of 50 patients who received non-operative treatment for the patella dislocation, 52 % had recurrent instability issues. Though these methods provide stability and relief to the patient, they result in redislocation rates ranging from 15-44 % [31]. When these conservative methods fail to correct the instability at the knee, surgeons opt for the operative procedures.

2.5.2 Operative methods

Operative procedures are usually recommended by a surgeon if the conservative methods fail to provide relief to the patient. A large number of procedures i.e. about 100 are available to treat the patellar instability, but no technique produced results to suggest that it was more superior and advantageous when compared to the other [31]. Each of them had its own benefits. The commonly followed techniques are the MPFL reconstruction for chronic cases, the MPFL repair for acute cases, lateral release, tibital tubercle transfer, trochleoplasty and medial repair.

i. MPFL repair and reconstruction: This technique provided a favorable outcome for patellar instability in studies conducted by Smith et al. (2007), Buckens et al. (2010) and Bitar et al. (2012). Graft materials were used to replace the torn ligament in chronic cases in their studies. Owing to the stiffness of the graft material used for replacing the torn ligament, lateral translations were restricted when compared to the native and sectioned MPFL. In acute cases, the damaged ligament was repaired with an arthroscopic procedure.

ii. Tibial tubercle transfer: This technique addresses the patellar instability problem by changing the Q-angle [23]. The tibial tubercle is shifted either medially or anteromedially. Transferring the tibial tubercle to a medial position reduces the pressures on the lateral compartment of the patella's articular cartilage [98]. This procedure is recommended for instability and pain due to maltracking of the patella [31].

iii. Trochleoplasty: Trochleoplasty addresses the clinical condition of trochlear dysplasia, in which the trochlear groove on the anterior aspect of distal femur has less than 3 mm depth [23]. The flat trochlear groove present in the central area is deepened by removing a portion and increasing the slope of the sulcus. This provides a potential space for patella to be fit into the trochlear groove and increased the stability.

iv. Lateral release: This technique involves the release of the tight lateral retinacular structures pulling the patella [23]. This procedure is usually not performed alone [22, 31].

v. Medial repair: The torn medial structures stabilizing the patella are repaired with this technique [31]. Along with realigning the dynamic medial stabilizer VMO, the MPFL is also repaired if found to be damaged.

2.6 Patellofemoral joint coordinate system

The joint coordinate system developed by Grood and Suntay (1983) was applied to the patellofemoral joint to measure the kinematics. This coordinate system is easily understood by clinicians. It can be applied to diagnosis of joint disorders, treatment and to study locomotion as anatomical landmarks are used for defining the axes along which the kinematic parameters are measured.

The Grood and Suntay coordinate system, when applied to two bodies involves a fixed axis in each of them and a floating axis, which is not fixed but moving in relation to both the bodies. Coordinate systems (Figure 2.10) are defined on both the bodies and then body fixed axes are taken to define the relative translations or rotations between the two bodies.

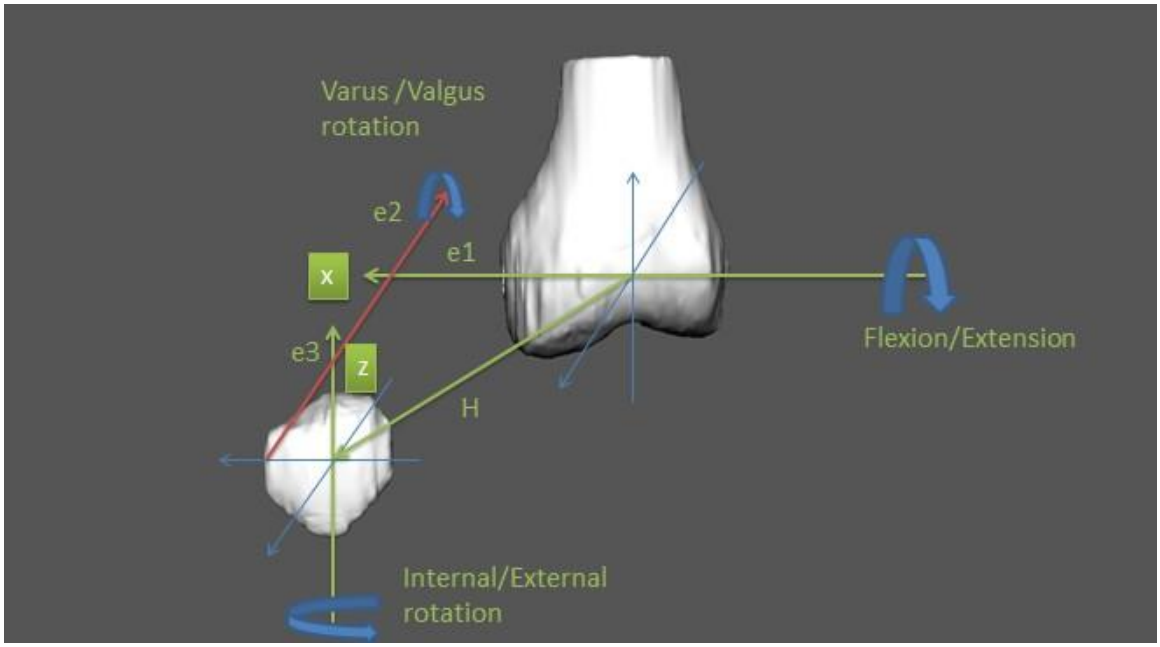

Figure 2.10: Joint coordinate system for the patellofemoral joint developed using the Grood and Suntay coordinate system.

For the femur, the epicondylar axis running through the most medial and lateral points is defined as the femoral X-axis (X_F). The femoral reference point (P_F) is defined midway between these two points. Two points are digitized proximal to P_F, along the midline of the femoral shaft on the posterior surface. The anterior-posterior axis, i.e. Y-axis (Y_F) is defined as the axis mutually perpendicular to the epicondylar axis. The femoral mechanical axis i.e. Z-axis (Z_F) is defined as the cross product of the anterior-posterior (Y_F) and the epicondylar axis (X_F) running along the proximal and distal directions.

For the patella, the x-axis (X_P) is defined as the axis passing along the most medial and lateral points. The z-axis (Z_P), i.e. the patellar mechanical axis passes

through the midpoint of the medial-lateral axis (patellar reference point P_P) and the most distal point on the patella. The cross product of X_P and Z_P is defined as the anterior-posterior axis of the patella, i.e the y-axis (Y_P).

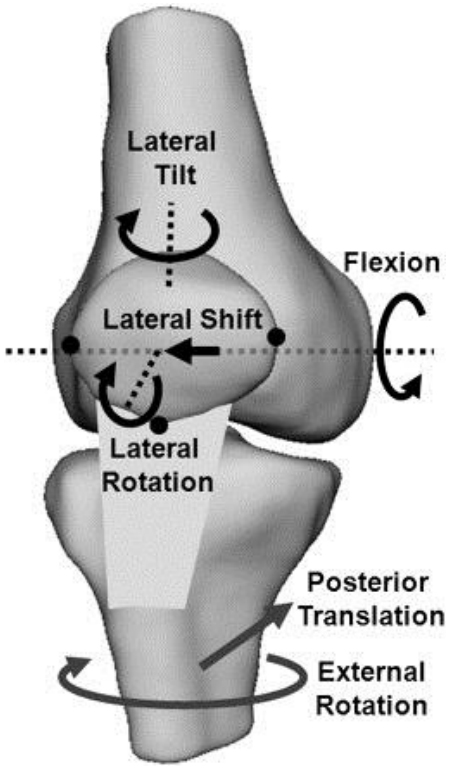

Figure 2.11: Rotations and translations at the knee (of the structures femur, patella and tibia).

Used with permission from Elias JJ, Kirkpatrick MS, Saranathan A, Mani S, Smith LG, Tanaka MJ. Hamstrings loading contributes to lateral patellofemoral malalignment and elevated cartilage pressures : An in vitro study. Clin Biomech. 2011; *26*(8): 841–6. [62]

With the coordinate systems defined for both the bodies, body fixed axes are chosen. The epicondylar axis i.e. X_F is taken as the femoral body axis (e1) and the patellar mechanical axis, i.e. Z_P is taken as the patellar body axis (e3). The floating axis, i.e. e2 is mutually perpendicular to these two axes. As shown in Figure 2.10, the vector H gives the relative position of the two body axes, i.e. the translation between the patella and femur.

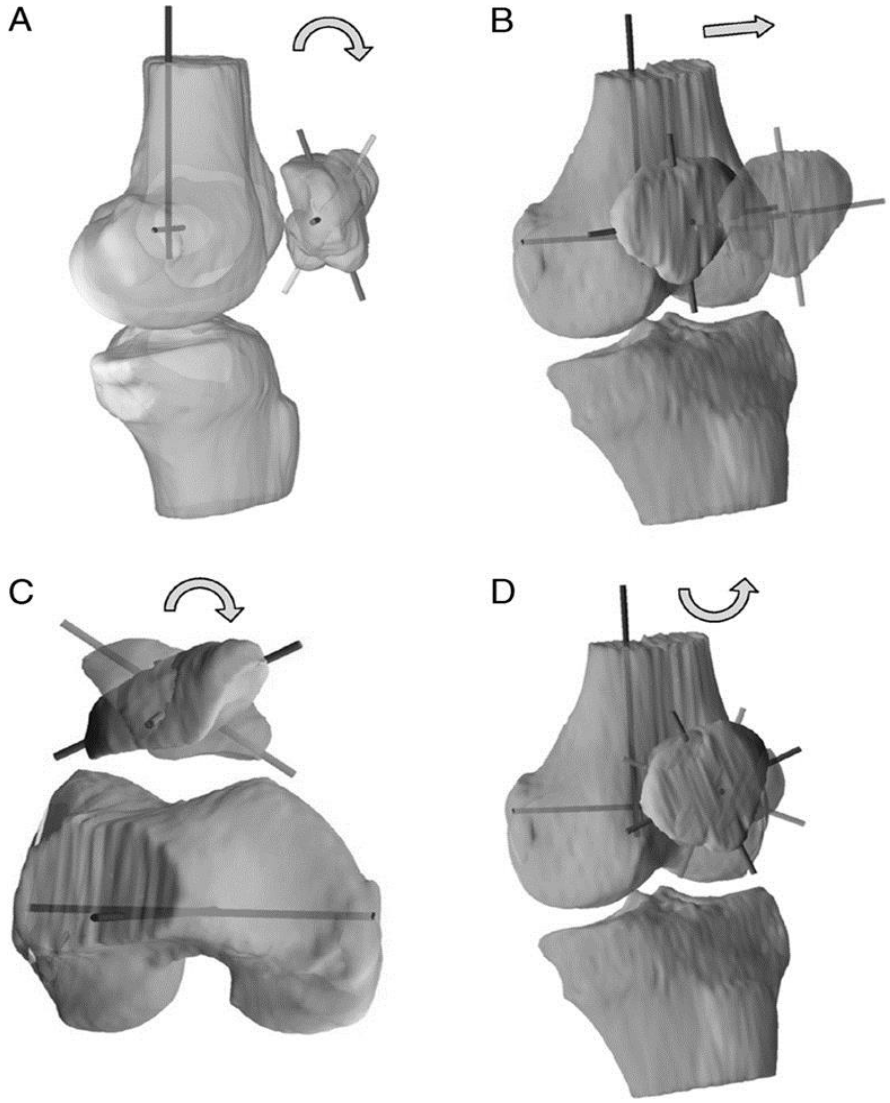

Figure 2.12: Illustration of the kinematics of the patella. A. patellar flexion in sagittal view, B. patellar shift in coronal view, C. patellar tilt in axial view, D. patellar rotation in coronal view (Positive in the direction of the arrow).

Used with permission from Van de Velde SK, Gill TJ, Li G. Dual fluoroscopic analysis of the posterior cruciate ligament - deficient patellofemoral joint during lunge. Med Sci Sports Exerc. 2009; 41(6): 1198-205. [65].

The six degrees of freedom in the present study are focused on the patellofemoral motion. Flexion / extension occurs about the epicondylar axis of the femur. While the internal / external rotation is measured about the patellar

fixed axis, the varus / valgus rotation is measured about the floating axis (Figures 2.11, 2.12). The translation of the patella along the medial-lateral directions is along the epicondylar axis of the femur, anterior is along the anterior-posterior axis and the distraction is along the superior-inferior axis, i.e. the patellar body axis.

2.7 Finite element analysis in biomechanics

In vitro experimental studies do not provide the complete details such as stresses and forces acting on the tissues to describe the behavior of the articular joint (or a system). FEM is regarded as a mathematical tool to simulate and parametrically study the behavior of a system. When applied to human joints in biomechanical studies, it offers the possibility to obtain the pressures and other forces acting on the tissues like articular cartilage and ligaments while simulating their dynamic behavior, but requires validation with an experimental study [81, 83]. Validation is necessary so that the results obtained from these simulations can be verified and accepted for further analysis. Modeling is performed with the help of mechanical properties of tissues, bones and cartilage structures available through the extensive literature. Changing a particular parameter in the model being developed for simulations influences the behavior of the system. FEM helps in studying these effects with reduced time and computational costs [66].

Mesh convergence analysis performed in a finite element study helps in deciding the appropriate element number to be used for the structures. To perform simulations and analyze the results with sufficient accuracy and to follow a good practice of finite element methods, it is necessary to check and ensure that

changing the mesh size does not influence the results obtained. An appropriate element size (in turn the element number) is to be decided before performing an analysis.

2.8 Previous studies

In vitro cadaver studies were conducted to determine the influence of the MPFL on the patellofemoral kinematics and the stability of the patella. Zaffagnini et al. (2013) measured the kinematics of the patellofemoral joint with the intact and resected MPFL conditions. They observed that with the intact MPFL, there was a medial shift of the patella. This medial shift was absent in the MPFL resected condition [58]. Beck et al. (2007) measured the contact pressures and the patellar translation with intact the MPFL and after a reconstruction with the semitendinosus graft. They found that the lateral translation of the patella was greater with the resected MPFL than with the intact ligament. Reconstruction with a graft and applying low graft tension lowered this lateral translation and stabilized the patella [59]. Philippot et al. (2012) studied the patellar tilt and patellar translation with the intact MPFL and a reconstructed graft with tension values 10 N, 20 N, 30 N and 40 N. They reported that 10 N was sufficient to restore the normal kinematics of the patella with the graft [97]. Dynamic and static MPFL reconstruction procedures were studied by Ostermeier et al. (2007). They observed that there were kinematic changes of the patella with the intact MPFL and the two types of reconstruction procedures.

Shah et al. (2012) developed finite element models of cadaver knee specimens to study the changes in the pressure and kinematic parameters with varying

hamstrings loading. The model as shown in Figure 2.13 included the femur and patella along with the spring representations for the quadriceps muscles, patella tendon, and the MPFL and meniscal ligaments. The models were validated with the results from an experimental in vitro study. In another study, subjects with patellar dislocation who had recurrence after the conservative treatment were enrolled. Feng et al. (2013) used the models reconstructed from the MRI scanning before and after the surgical procedures and measured the patellofemoral kinematics using the Grood and Suntay (1983) coordinate system to characterize the changes.

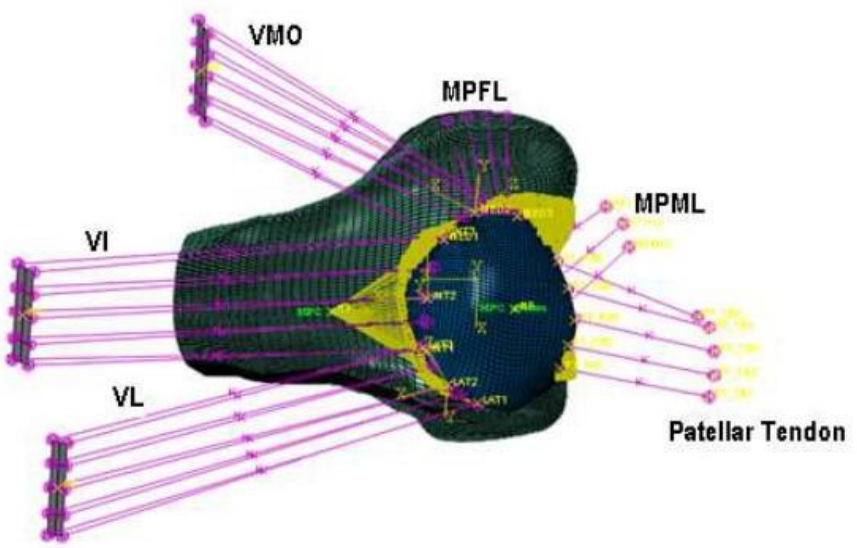

Figure 2.13: Finite element model developed by Shah et al (2012).

There was no previous evidence of a computational modeling study looking at the influence of the MPFL on patellar stability. For the proposed study, subject

specific computational models were developed based on FEM to study the patellofemoral kinematics. The subject had a dysplastic knee and patellar instability. Reconstruction of the ruptured MPFL was performed to correct the instability. The main goals were to validate the FEA models with the in vivo imaging analysis study results from Feng et al. (2013), study the patellar kinematics and use these models to quantify the effects of varying the MPFL graft attachment points.

CHAPTER III

MATERIALS AND METHODS

3.1 Overview

The kinematics of the knee and the influence of the reconstruction of the MPFL on the articular cartilage were studied using computational models of the patellofemoral joint. The required knee geometry was obtained from 3D image reconstructions using the MRI of a subject taken before the reconstruction surgery. The models were built at six flexion angles – 15°, 19°, 22°, 36°, 49° and 57°.

3.2 MRI image acquisition and reconstruction

3.2.1 MRI scans

The computational knee joint models were based on the data obtained from patient specific MRI data. The subject (female, 16 years) had a dysplastic left knee and an MPFL tear. Two types of MRI scans, a high resolution and a low resolution, were taken using a 3.0 T Siemens Magnetom Skyra MRI scanner (Akron Children's Hospital). These MRI scans were taken before and after the ligament reconstruction surgery. A high resolution scan was taken with the knee extended (TE = 10 sec, TR = 3000 sec, slice thickness = 1.5 mm, flip angle = 180°, scan time = 7.32 minutes). Low resolution scans were taken at 6 different

flexion angles (TE = 8.7 sec, TR = 725 sec, slice thickness = 2 mm, flip angle = 150°, scan time = 30 seconds), at angles 15°, 19°, 22°, 36°, 49° and 57°. Since the subject had instability at the knee, it was difficult to position in a flexed position for long durations as it would result in pain at the joint. To obtain the positions of the bones and cartilage at the flexed positions, low resolution scans were taken with flexed knee positions for short durations. A high resolution MRI scan of the extended knee taken for a longer duration provided a detailed view of all the features of the bones and cartilage.

During the MRI scan, the patient was asked to rest her foot on the footplate of a loading frame and push against an elastic band. This induced the quadriceps muscle loading. This loading frame had only non-metallic parts and was designed to assist the subject when the knee was in a flexed position between 0 and 60° by resisting knee extension.

This frame had supporting and loading components. Supporting components including a back plate and padded straps were used so that the frame and the torso of the subject were held and supported in a fixed position. Figure 3.1 shows a foot plate provided in the loading frame as part of the loading mechanism, where the subject's foot was positioned with the help of straps. This foot plate was supported by the plastic rollers in the grooves of the base and was connected to the frame using an elastic band. Spacers were used between the back wall of the frame and the foot plate. These blocks helped in adjusting the distance between the foot plate and the wall, which in turn influenced the

displacement of the elastic band and the applied force. The force applied on the loading frame was calibrated using a handheld force transducer (Force One FDIX, Wagner Instruments, Greenwich, CT) and the displacement of the footplate was connected to this force measurement. A more detailed picture of the position of the subject is shown in Figure 3.2.

Figure 3.1: The loading frame used during the MRI scan procedure.

The MPFL reconstruction surgery was performed with a semitendinosus tendon as the graft for the ligament. Post-operatively, the same procedure was followed to obtain a high resolution MRI and low resolution MRI scans at the six flexion angles. The positions of the bones and cartilage structures at flexed knee positions were obtained by shape matching and aligning the reconstructions of high resolution and low resolution MRI scans.

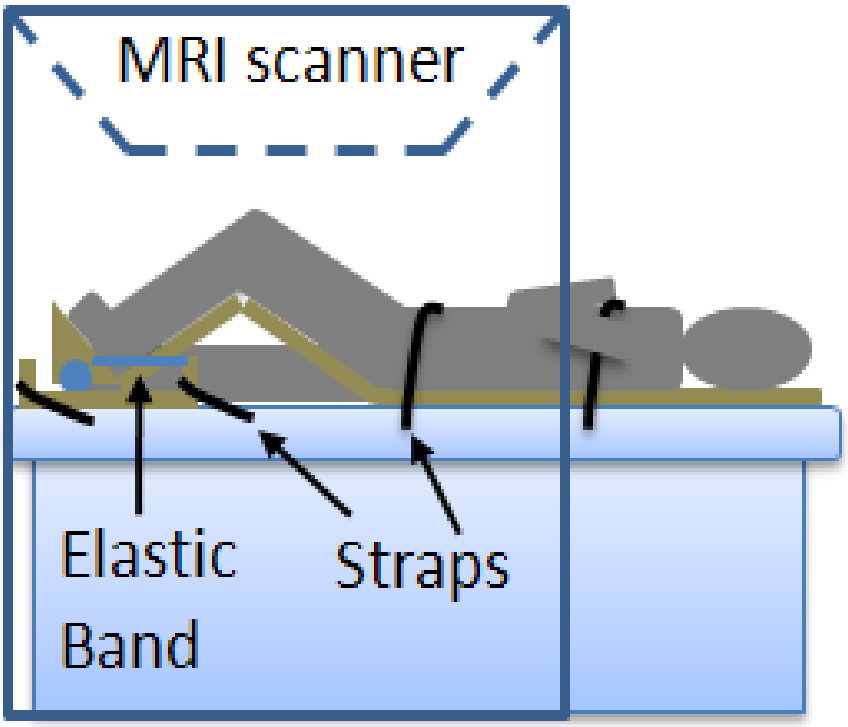

Figure 3.2: Patient positioning during MRI scan procedure and the jig [25].

3.2.2 Reconstruction and alignment

Segmentation of MRI images was performed manually using the medical imaging, rendering and 3D visualization software 3D-Doctor (Able software Corp). This segmentation was done to trace the structures and provide the necessary anatomical geometry for generating the finite element meshes.

The femur, patella, patella cartilage and femur cartilage were traced manually in each slice of the MRI data using the boundary tools (Figure 3.3). After the segmentation of the structures, surface rendering function of 3D-Doctor was used to create the 3D polygonal surface meshes. Stereolithography (‘.stl’) files were created, so as to import the structures into CAD processing software to develop the finite element meshes using a mesh pre-processor.

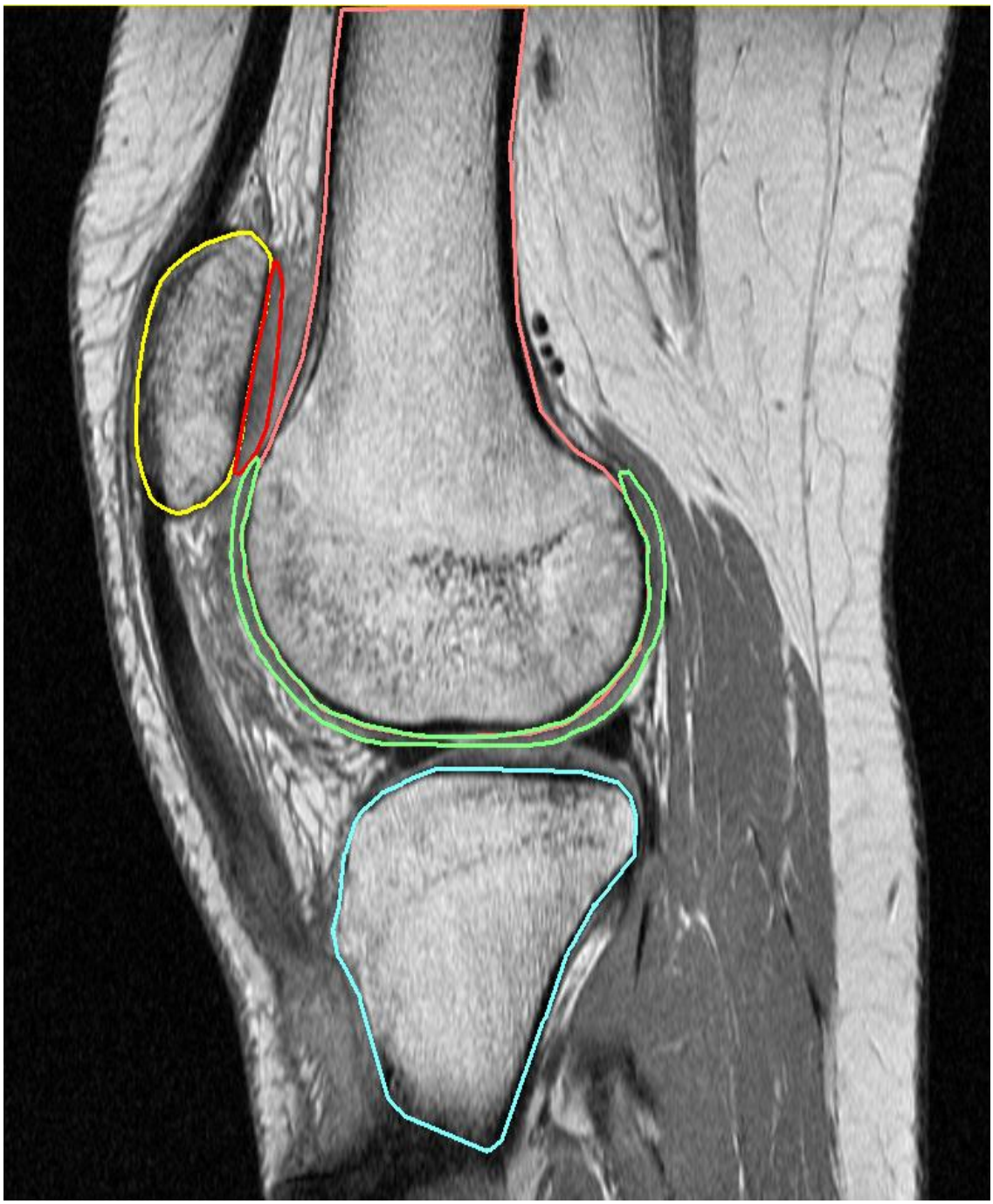

Figure 3.3: High resolution MRI scan of extended Knee.

Smoothing and other surface improvement functions were carried out by importing the stereolithography files into VR-Mesh (VirtualGrid). This operation would remove any uneven features on the surface of the structure. In AC3D (Inivis), anatomical landmark points based on the patellofemoral joint coordinate

system by Grood and Suntay (1983) were digitized on the models from high resolution scans. The landmarks digitized were the most medial and lateral points and the most distal point on the patella. On the femur, the most medial and lateral points and two proximal points along the femoral shaft were digitized. These digitized landmarks were necessary to calculate the kinematics of the patellofemoral joint. The high resolution scans (Figure 3.3) provided a detailed view of the anatomical features, while the low resolution scans (Figure 3.4) provided information regarding the positions of the bones and cartilage. Structures from high resolution, unloaded scans were aligned with those from the low resolution, loaded scans. In MATLAB (MathWorks, Natick, MA), these low resolution models were then aligned by shape matching to the high resolution models using iterative closest point (ICP) algorithm with kinematics obtained from the landmarks [8]. The ICP algorithm used two point cloud meshes as input and resulted in the rotation matrix R and translation matrix T which provided the best possible alignment match for the two structures [8].

Figure 3.4: Low resolution MRI scan of flexed knee.

3.3 Model development

A finite element model of the patellofemoral joint was built based on a number of assumptions. The mesh, the main ground for the finite element model development, was initially developed based on the geometry of the traced

structures. This mesh was then imported into the commercial finite element solver, ABAQUS/CAE (Dassault Systemes) [40], where the model development involved three different stages:

a) Pre-processing (modeling with subject specific loads and assembly)
b) Simulation of the models
c) Post-processing of the finite element results.

The parts were created in the part module. The representations of these parts were taken into the assembly module; muscles and graft were modeled in the interaction module and loading and boundary conditions were defined in the load module. The type of the analysis was defined in the step module.

3.4 Parts - mesh generation

The stereolithography files obtained from the 3D-Doctor software were used for the generation of finite element meshes of the knee structures. Finite element meshes for the knee structures were generated using a mesh pre-processor.

3.4.1 Finite element mesh generation (TrueGrid)

TrueGrid (XYZ Scientific Applications, Livermore, CA) [39], a commercial finite element mesh pre-processor was used for the mesh generation. Surface meshes and volumetric meshes were generated for the bones and cartilage, respectively. The surface mesh structures for the bones were comprised of linear quadrilateral elements, while the volumetric mesh structures for the cartilage were comprised of linear hexahedral elements. Though hexahedral mesh was difficult to construct in terms of amount of time consumed and experience it takes to generate, it was

preferred over the tetrahedral mesh. Compared to the tetrahedral elements, hexahedral mesh offered a higher accuracy, particularly for biomechanical soft tissues like cartilage structures in which the strains were expected to be high [91].

In TrueGrid, to create mesh for a 3D CAD structure, a crude block mesh was constructed first. The faces, edges and corners of this block mesh were modified according to the 3D shape being meshed and then a projection was done to exactly match the shape and to avoid missing any small details. Three phases were followed for the creation of finite element meshes.

3.4.1.1 Control phase

In this initial phase of TrueGrid, text and menu windows were displayed. While the text window provided the space for manually entering the commands along with the parameters, the menu window displayed the list of commands available for the particular phase of the code. The geometry of the structures to be meshed i.e. the '.stl' files of femur, femur cartilage, patella and patella cartilage generated from 3D-Doctor were imported into TrueGrid as CAD features.

3.4.1.2 Part phase

This phase was started by issuing a block command to generate either a single block or multi block. In addition to the text and menu windows, the physical window (displays the crude block mesh and the CAD geometry imported), the computational window (displays the logical blocks of the crude block mesh using a multi block), and the environment window (provides the GUI for manipulating

the view and selecting what appears in the physical and computational windows) appeared in this part phase.

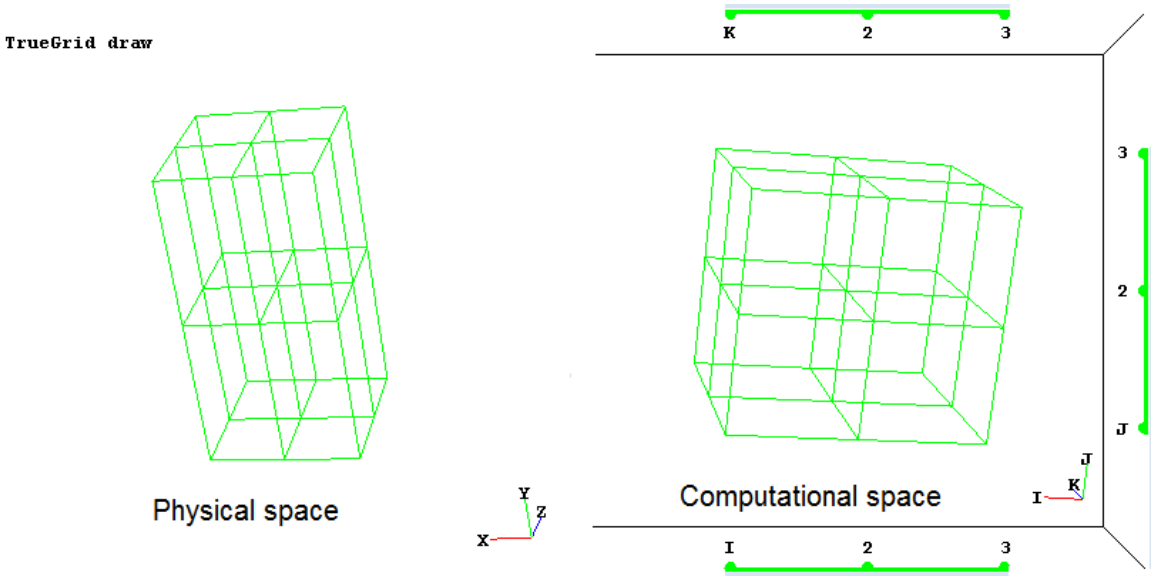

Figure 3.5: physical mesh and computational mesh.

The computational window (Figure 3.5) displayed a multi block or single block with reference to the i j k coordinate system. The actual mesh had x y z as the reference coordinate system. Index bars along i, j and k directions helped in selecting either a face or an edge or a corner of the physical mesh (i.e. mesh selection through its correspondence with nodes of the computational mesh). Geometric and topological operations were performed on the crude block mesh in the physical window using the multi/single block in the computational window to construct the required mesh. The computational mesh was used for selecting the regions and did not move when any geometrical or topological operation was performed on the physical mesh. The edges, faces and corners of the block mesh were modified by positioning, projecting, deleting or smoothing to suit the shape of the 3D CAD feature.

The closest point algorithm was then used to project the crude block mesh onto the surface of the imported 3D CAD structure (Figure 3.6). The projection of the crude block mesh onto the surface of the CAD feature created a coarse mesh for the structure. To increase the mesh density and to create a finer finite element mesh, seeding was performed along the i, j and k directions of the computational mesh. Uniform smoothing was performed to have elements of uniform dimensions along all regions (Figure 3.7).

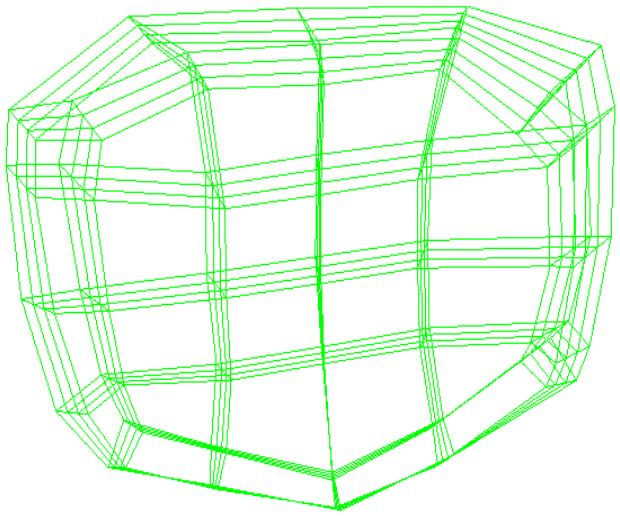

Figure 3.6: Physical crude mesh shaped and projected onto patella cartilage.

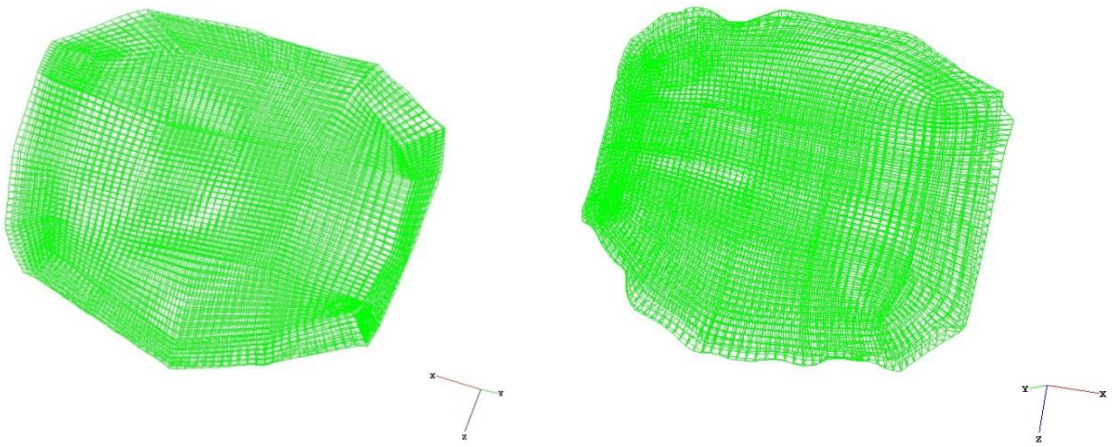

Figure 3.7: Seeding done on crude mesh (left), uniform smoothing after seeding in physical space (right).

A cube was used as the multi block for building the finite element meshes for bones and cartilage. For the femur and patella, surface meshes were constructed by deleting all internal elements of the cube and projecting the surface of the cube onto the surface of the bones. Volumetric meshes were built for the cartilage structures. For the patella cartilage, a butterfly mesh technique was used while the femur cartilage mesh was built with the cube constructed initially and geometrical operations performed to match the shape. The complex shape and curves of the patella cartilage were best represented with a mesh built using the butterfly technique. With this technique, the corner blocks of the cube were deleted. Figure 3.8 shows the elements deleted at the corners in the mesh displayed in computational space and the mesh for patella cartilage developed using a butterfly technique in the physical mesh. To cover the deleted area of the mesh, the elements whose adjacent portions were deleted at the corners were merged by specifying one as master and the other as slave. This transformed the

outer boundary into the form of a circle instead of a regular polygon shape. For curved and complex surfaces like patella cartilage, this technique was extremely useful to capture every small detail. Three layers of elements were ensured along the thickness of the cartilage finite element meshes. This provided a better view of the deformation when interaction occurred.

Mesh quality for the elements was checked using the measures of orthogonality and volume of the element. The orthogonal quality measured the deviation of the angles between adjacent faces of a quadrilateral from 90°. The volume of the element was always kept positive above zero and any negative volume elements were avoided. These measures were necessary so that a quality finite element mesh was produced for analysis in the finite element solver.

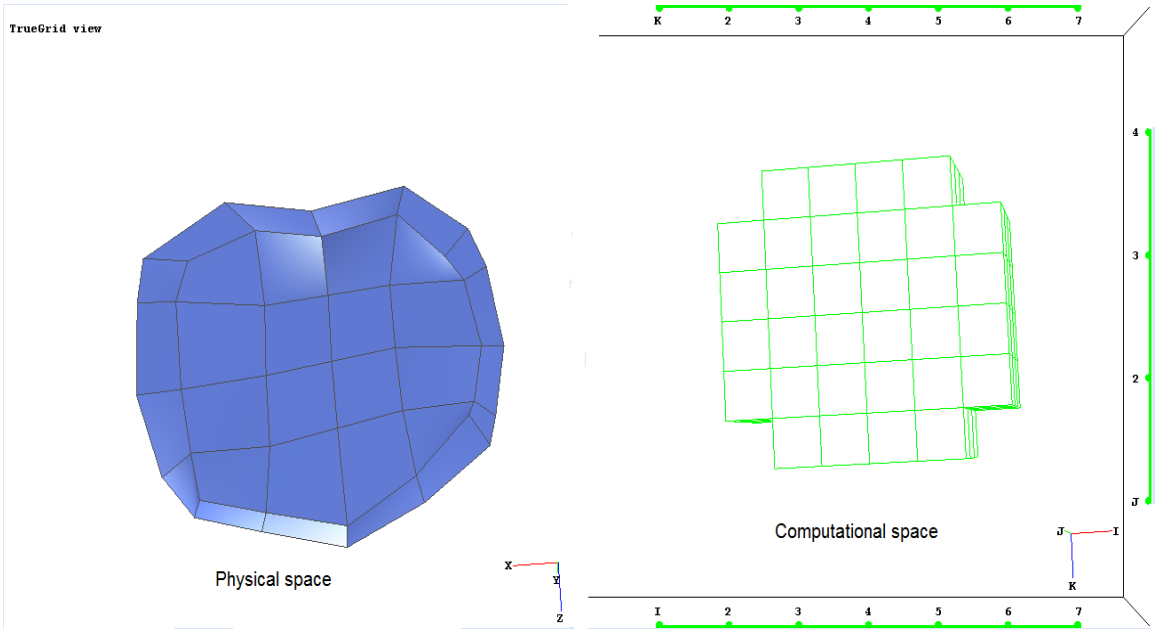

Figure 3.8: Butterfly technique for patella cartilage.

3.4.1.3 Merge phase

Once the number of elements for the mesh and the quality of the mesh created in the part phase were adequate, the process was shifted to the next phase by issuing a “merge” command in the text window. The computational mesh did not allow modifying the physical mesh in this phase. The input file necessary for the analysis in ABAQUS/CAE was written using the “abaqus write” command.

Surface meshes comprising linear quadrilateral elements, i.e. R3D4 (4-noded, rigid elements) were generated for the bones (Figure 3.9). Volumetric meshes comprising hexahedral elements, i.e. C3D8 (8-noded, deformable elements) were generated for femur cartilage and patellar cartilage (Figure 3.10). The four meshes were then imported as a single model in the part module of the ABAQUS/CAE for further model development. An input script file (Appendix A) was written externally for including the ‘.inp’ files of the knee structures generated by TrueGrid.

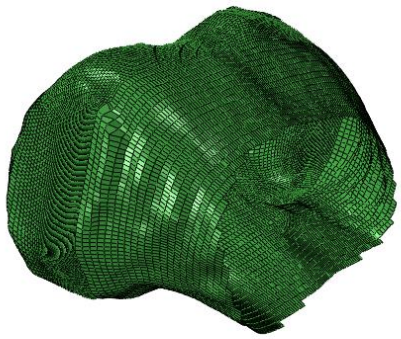

Figure 3.9: 4-noded quadrilateral elements (R3D4) for bones.

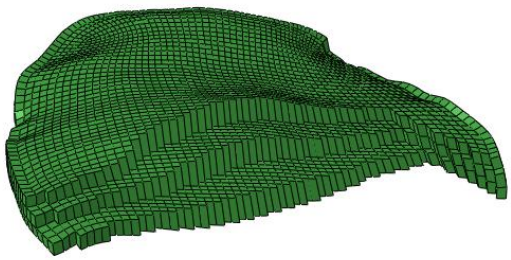

Figure 3.10: 8-noded hexahedral elements for cartilages (C3D8).

3.4.2 Other supporting structures

The quadriceps muscles were represented using spring elements (10 elements each for the muscle bands VI, VL and VMO). To support these spring elements at the muscle origination points, a rigid body was constructed. A 3D discrete rigid shell planar plate was built with dimensions 20 mm X 10 mm (Figure 3.11). A reference point was specified at the center of the body to accommodate for the rigid body reference point. To create the reference points for the spring elements at the muscle origin points, the plate sketch was partitioned into 10 equal parts.

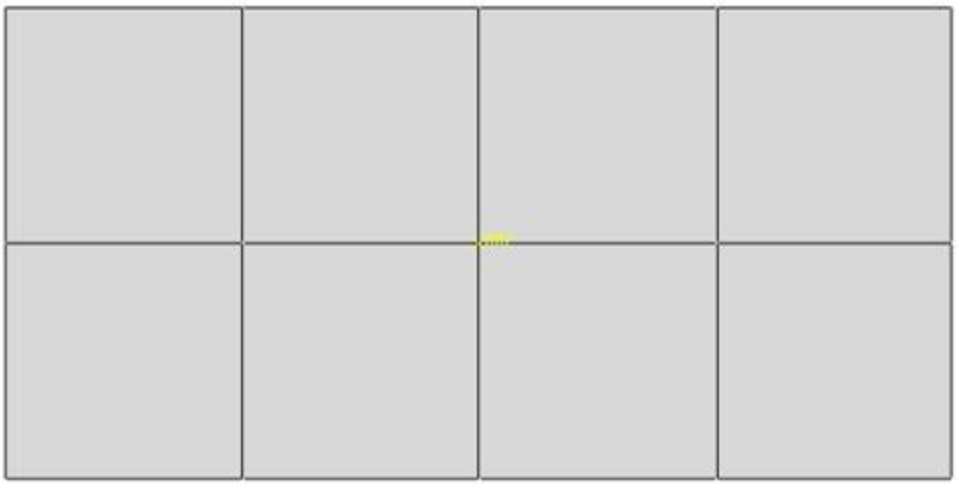

Figure 3.11: 3D rigid shell planar plate for support at the muscle origin points with rigid body reference point.

In the assembly and interaction modules, reference attachment points were created on these planar plates to support the linear tension only spring elements representing the muscle bands VI, VL and VMO of the quadriceps muscle group at their origin points. In the loading module, these rigid plates were used to specify the loads acting through the spring elements on the patella.

3.5 Material properties

Previous studies performed using finite element model simulations of the patellofemoral joint and other structures indicated that a model in which all geometries were modeled as deformable, involved significant computational time to solve and post-process the results [51]. To reduce the complexity of the finite element models developed and to increase the computational efficiency, the mesh structures based on the geometry of the femur and patella were modeled

as rigid [51, 74] (Figure 3.9). These rigid bodies did not have element level calculations in the finite element models [40].

Articular cartilage is porous and has 80% fluid phase by wet weight along with solid and ion phases. It exhibits viscoelastic and time dependent behavior under a constant deformation load. In normal articular cartilage, the permeability being very small, the majority of the compressive load support comes from the fluid compartment [27]. To account for the steady state response of the cartilage structures with low permeability, patella cartilage and femur cartilage were modeled as deformable isotropic elastic structures. A Young's Modulus of 10 MPa and a Poisson's ratio of 0.45 were used for the articular cartilage [37, 38].

3.6 Assembly module

Each of the individual structures imported into the part module as distinct orphan meshes were positioned with reference to their own coordinate systems. A representation of orphan meshes (meshes generated from a mesh pre-processor) with the geometry and orientation information was taken in the assembly module. They were positioned with reference to a global coordinate system in which the modeling was done to perform an analysis. Other parts to support the muscles were also represented in the assembly module to start creating the interactions and imposing loading conditions on them. The finite element models of the patellofemoral joint were built after the alignment procedure. Alignment of the high resolution structures with those of the low resolution was performed at knee flexion angles 15°, 19°, 22°, 36°, 49° and 57°.

Thus, with the help of the alignment process of the structures, the original patellofemoral joint model was modified to different flexion angles.

3.6.1 Parts

One representation of each of the orphan meshes corresponding to the femur, patella, femur cartilage and patella cartilage was used in the assembly module for the patellofemoral joint finite element model at a particular flexion angle. These representations were dependent on the orphan meshes for anatomical geometry and coordinate system. Under circumstances where there were any model convergence problems, it was necessary to slightly change the node positions and geometry of the structures. These changes made on the orphan meshes were easily reflected on the representations (dependent) in the assembly module.

In addition to orphan meshes of the knee structures, 3 representations of the 3D discrete rigid shell planar plate were also taken as dependent parts in the assembly module with respect to the global coordinate system. Figures 3.12, 3.13 show the patellofemoral joint assembly in different orientations.

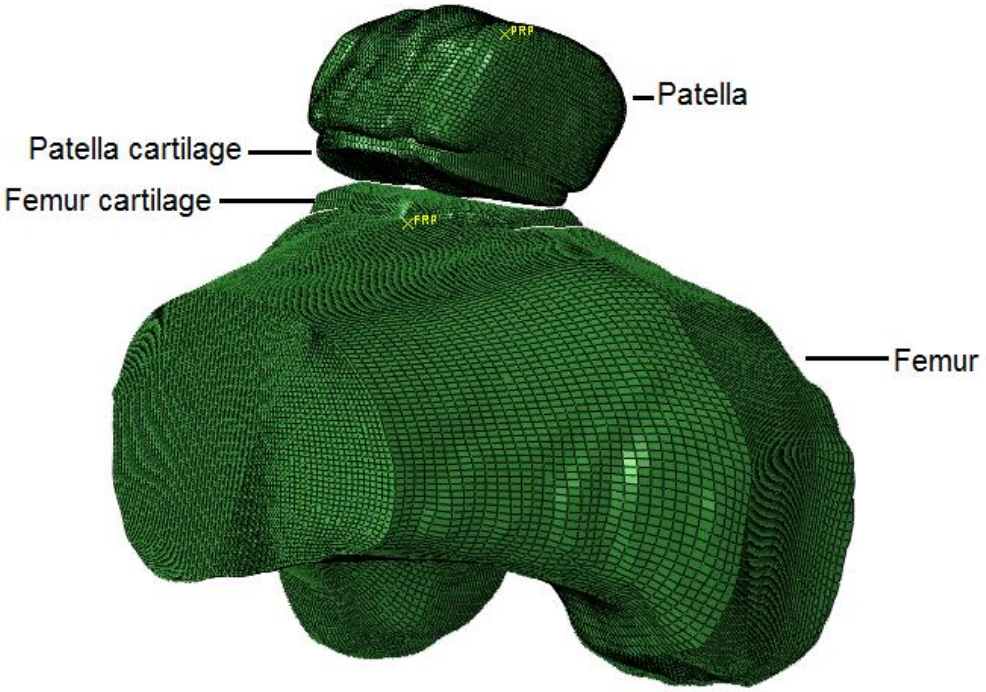

Figure 3.12: Assembly of the instances (FRP on femur stands for femur reference point and PRP on patella for patella reference point).

Figure 3.13: Side view of the assembly.

3.6.2 Reference points and datum coordinate systems

To constrain the femur in all directions and to specify the motion of the patella, reference points were created for the rigid bodies in the part module (FRP on the femur and PRP on the patella). Along with specifying the attachment points for the linear springs on the patella and the tibial trochlea, reference points (RRP) were also created on the planar plates.

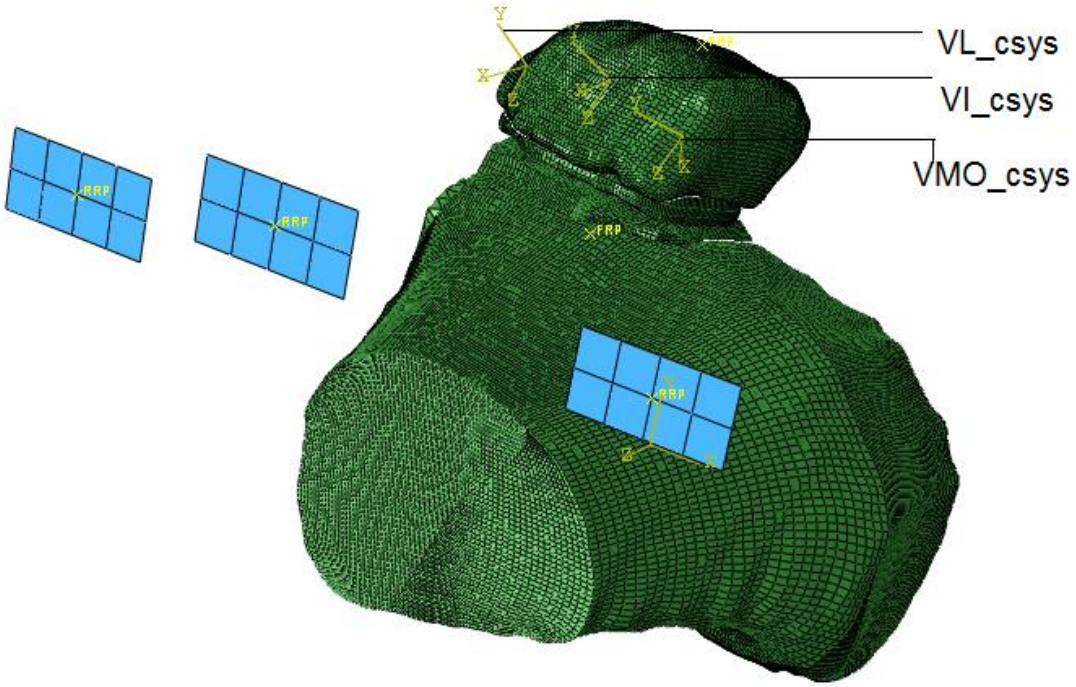

Figure 3.14: Rigid body reference points and datum coordinate systems VI_csys, VL_csys, VMO_csys.

To easily create the interactions and specify the loading and boundary conditions in the next modules, datum coordinate systems were necessary and were created with respect to the global coordinate system. Three rectangular datum coordinate systems VI_csys, VL_csys and VMO_csys (Figure 3.14) were created near the patella attachment points of the quadriceps muscles. They were

oriented with their X-axes directed towards the linear spring origin point on the shell planar plate from the patella insertion point.

3.7 Interactions

With the use of this interaction module in ABAQUS/CAE, the critically important surface-to-surface contact was defined between the patella cartilage and femur cartilage in addition to defining the interaction properties to depict the behavior of the synovial fluid between them in the knee joint.

3.7.1 Node sets

To define the constraints between the bones and cartilage structures as will be explained in the next sections, node sets were defined on the deformable structures. On the back surface of the femur cartilage and on the front surface of the patella cartilage (i.e. the surfaces with which the cartilage has an articulation with the bones), all the nodes were selected to create a 'Pcart_set' and 'Fcart_set', respectively (Figure 3.15).

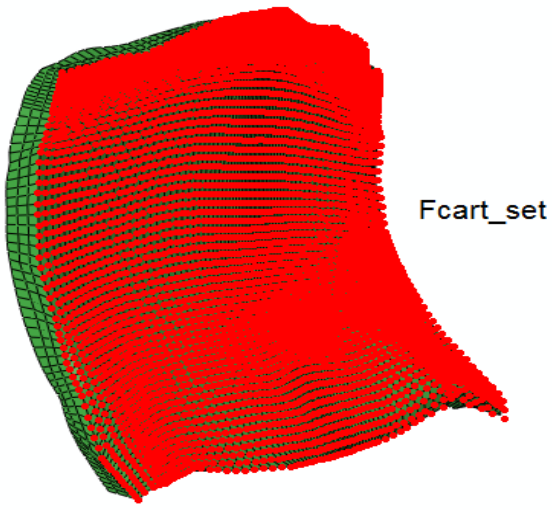

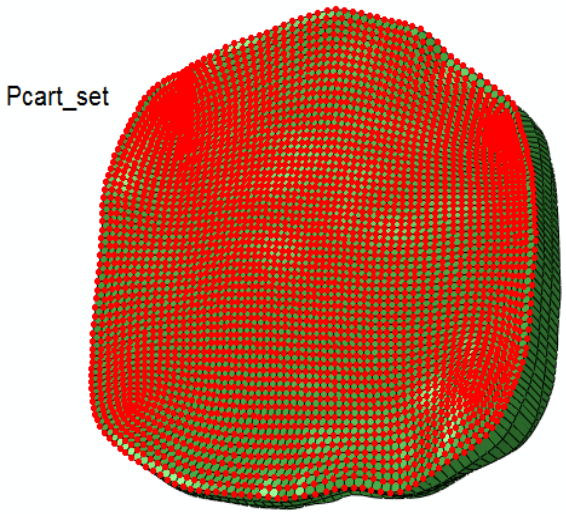

Figure 3.15: Femur cartilage (top) and patella cartilage (bottom) node sets.

3.7.2 Element surfaces

Element-based surface definitions were needed in the finite element model to define the contact between the two cartilage surfaces. Similar to the method by which the node sets were created, element surfaces ‘Pcart_surf’ and ‘Fcart_surf’ were defined on the back surface of the patella cartilage and on the front surface of the femur cartilage, respectively by selecting the elements (Figure 3.16). These surfaces were necessary to define the master and slave surfaces of the contact analysis. Defining element surfaces on the regions that would not come into contact during the analysis increased the memory usage and computational costs. Only the elements on the front surface of the cartilage were selected.

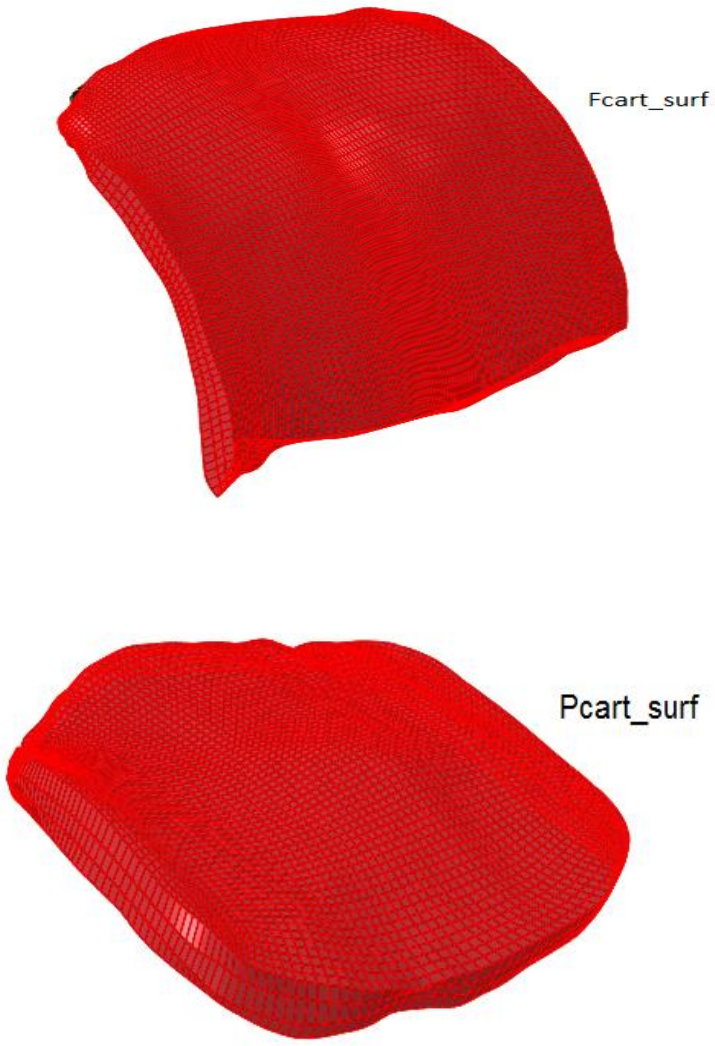

Figure 3.16: Element surfaces on femur cartilage (top) and patella cartilage (bottom).

3.7.3 Wire elements for the MPFL graft

Patellofemoral joint models were constructed at the six flexion angles from pre-op and post-op MRI data. The models differed in only the MPFL graft constructed between the femur and patella in the post-op models.

Two connector wire elements were created with attachment points on the femur near the adductor tubercle (taken from the reconstructions of post-op MRI data) and on the superior medial border of the patella to represent the MPFL graft

(semitendinosus tendon) (Figure 3.17). Uniaxial connector behavior (mimicking the spring behavior) was defined for the wire elements, so that they represented the graft properties [68]. The stiffness of the graft was 100 N/mm [63, 87] and was specified by selecting the elastic behavior for the connector elements.

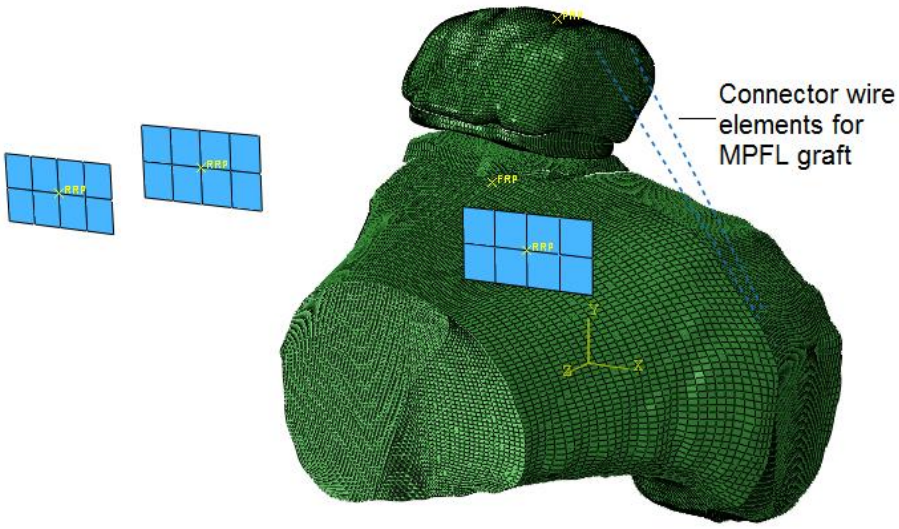

Figure 3.17: Connector wire elements representing the MPFL ligament graft.

Optimal attachment points for placing the graft were studied by using experimental and imaging techniques from previous studies [12, 45, 46, 47]. In the post-op MRI scans, it was observed that the two strands of the ligament graft were positioned at the superior and proximal medial border on the patella side. On the femoral side, the graft was positioned below the adductor tubercle near the medial epicondyle. Based on these positions, the two wire elements were adjusted between the femur and patella mesh structures.

3.7.4 Spring elements for muscles and tendon

Linear and tension only spring elements were used for modeling the quadriceps muscles and patella tendon to represent their elastic behavior. The muscle bands VI, VL and VMO were each represented by a set of 10 linear tension only spring elements oriented using the X-axis of the three datum coordinate systems VI_csys, VL_csys and VMO_csys, respectively (Figure 3.18). These elements had attachment points on the superior border of the patella and the three rigid shell planar bodies. The patella attachment points for the quadriceps muscle bands were obtained from the reconstruction of the structures (MRI data). For each quadriceps muscle band, spring stiffness of 1350 N/mm was given and was distributed equally between the 10 spring elements [95]. The orientation of the quadriceps muscle bands was derived from the lower limb model developed using SIMM (Software for Interactive Musculoskeletal Modeling) [96].

The patella tendon was represented by a set of 5 linear and tension only spring elements using the global coordinate system (Figure 3.19). Attachment points were on the distal border of the patella and on the tibial tubercle which were obtained through the reconstruction of the structures. A spring stiffness of 2000 N/mm was specified and was distributed equally between the elements (400 N/mm for each element) [41, 42, 95].

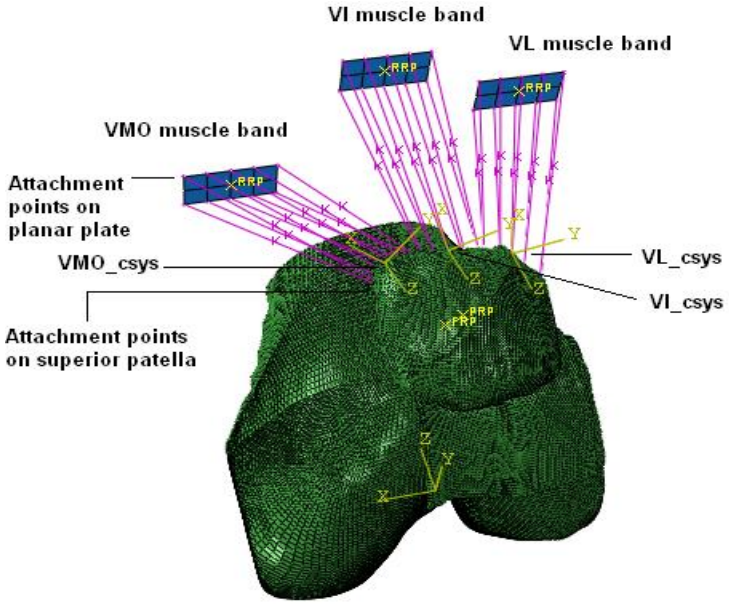

Figure 3.18: Linear spring elements representing quadriceps muscle bands.

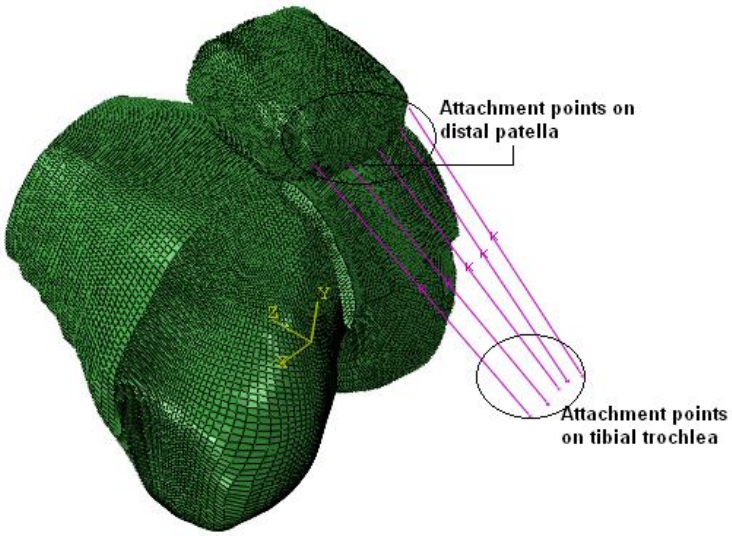

Figure 3.19: Linear spring elements representing patella tendon.

Pretension was used for the spring elements and the uniaxial connector wire elements so as to avoid any slack in them by specifying force-displacement relationships. These relationships were specified over a sufficiently wide range with necessary keywords for the spring elements [68]. The keywords (or options)

were specified in the ABAQUS input file with data corresponding to the elements and nodes and were used to describe the element connectivity in the finite element mesh and the type of analysis being run.

3.7.5 Master and slave surface for contact interaction

The two cartilage structures interacted with one another once the loads were applied through the linear springs. As such, element based surfaces were defined on them to run the mechanical contact simulation. Surface-to-surface contact was created between the two element based surfaces (Figure 3.20). Sliding and separation (due to lubrication behavior of the synovial fluid in the natural joint) along with arbitrary rotation was allowed by selecting the finite-sliding formulation.

Both the femur cartilage surface and patella cartilage surface were defined on deformable bodies. A master surface and slave surface were to be selected between the two for the contact pair. Even though the femur cartilage surface was larger than the patella cartilage surface, a symmetric master-slave method (two contact pairs) was used to treat each of the two surfaces as master surface and slave surfaces alternatively. This selection increased the computational cost, but it also increased accuracy when there was penetration between the two surfaces.

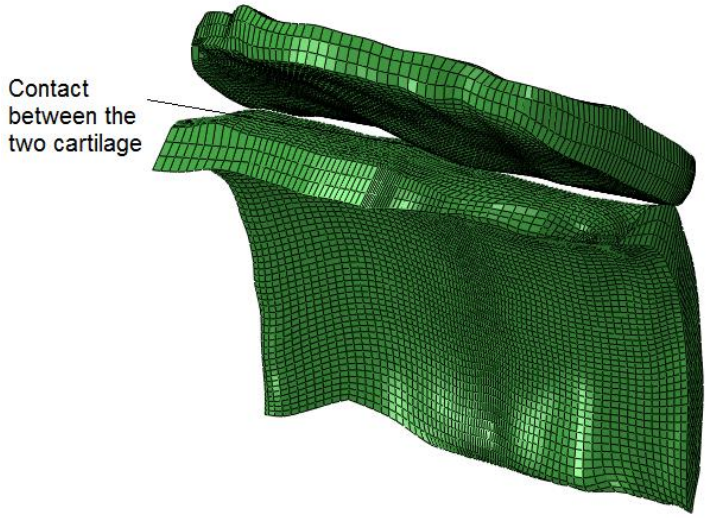

Figure 3.20: Contact between the two cartilage surfaces.

3.7.6 Contact interaction properties

The interaction between the two cartilage surfaces when the loads were applied on the patella through the quadriceps springs was defined with contact interaction properties through the normal behavior and the tangential behavior. These properties were applied to the master and slave surface contact pair defined previously.

A hard contact pressure over closure relationship was defined for the contact interaction between the two cartilage surfaces. This pressure relationship indicated that contact stresses and pressures developed only when the surfaces interacted with each other. No penetration was allowed at any location and there was no limitation to the magnitude of contact pressures that were developed when the surfaces interacted with each other. Once the two structures contacted during the first stage of the analysis, no separation was allowed.

Synovial fluid in the knee joint is responsible for the lubrication and in turn the frictional behavior of the articular cartilage. To account for this, a friction coefficient of 0.02 was defined between the cartilage surfaces through the tangential behavior - penalty friction formulation options [82]. The contact pressure developed between the two surfaces was proportional to the amount of penetration between the two contacting bodies with this penalty formulation [40].

3.7.7 Constraints

A bone is covered with cartilage at a joint, which implies that the displacement and rotation of the cartilage is restricted with the bone to which it is attached. This formed the basis for defining the multipoint constraint in the finite element model of the patellofemoral joint. As mentioned in the previous sections, node sets were defined on the back surface of the femur cartilage and on the front surface of the patella cartilage. The femur and patella were defined as rigid bodies and each rigid body had a 'reference point'. One multi-point beam constraint was defined between the femur reference point and the femur cartilage node set (Figure 3.21) while the other was between the patella reference point and the patella cartilage node set (Figure 3.22).

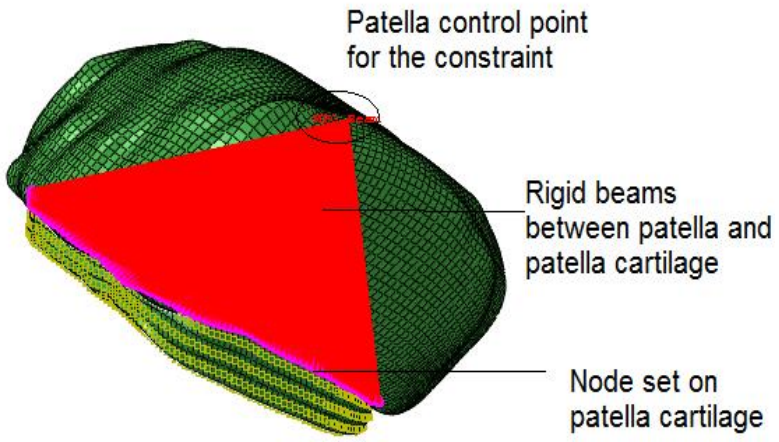

Figure 3.21: MPC beam constraint between patella and patella cartilage.

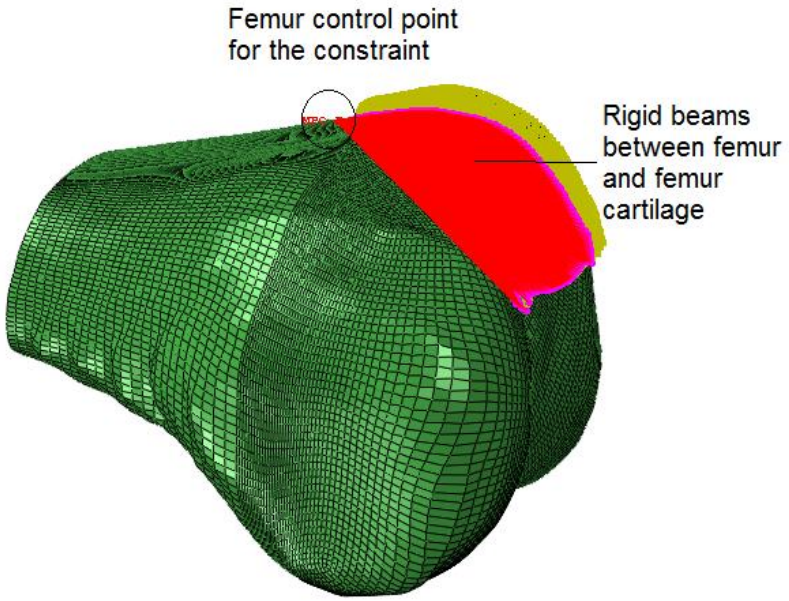

Figure 3.22: MPC beam constraint between femur and femur cartilage.

The multi-point beam constraint created a rigid beam between the rigid body reference point and the node sets of the deformable cartilage structure. This rigid beam related the translation and rotation in any degree of freedom of the rigid bone to the translation and rotation of the cartilage. Figure 3.23 depicts a view of the patellofemoral joint finite element model after the spring elements representing muscles and ligaments have been modeled. Interaction was specified between the patella cartilage and the femur cartilage.

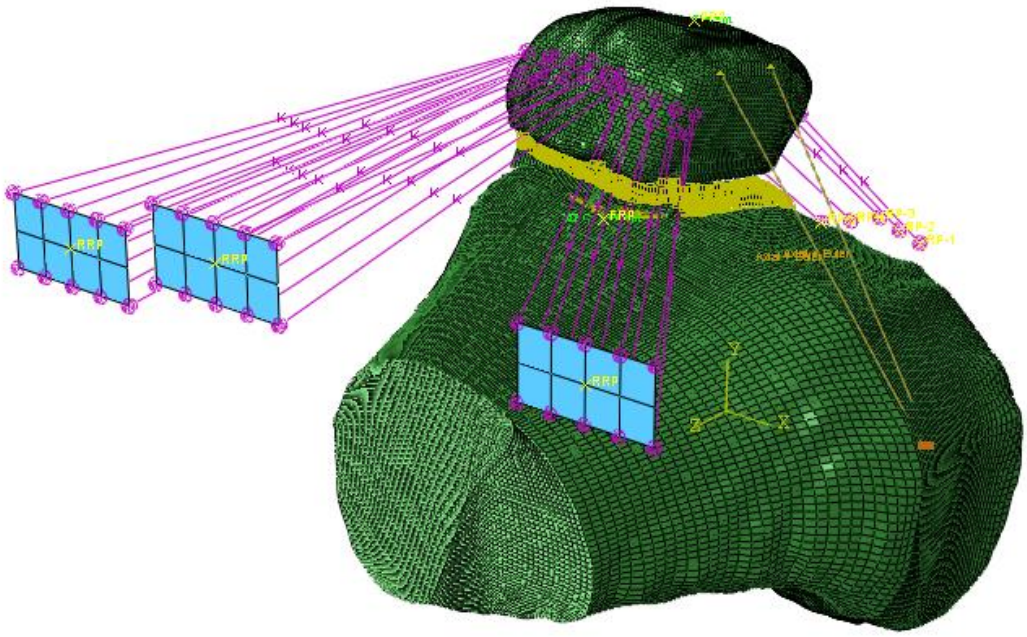

Figure 3.23: Patellofemoral joint finite element model with all the engineering features.

3.8 Analysis step module

In ABAQUS/CAE, static and non-linear geometric analyses of the patellofemoral joint finite element model were performed in two stages. The total computational

time for the analysis was 2 seconds; each stage had a step time of 1 second starting from 0. At the end of each stage, the model was in equilibrium with the conditions specified and the results were written to the output database.

3.8.1 Displacement step

Contact analysis with two bodies in contact before the start of the analysis posed significant convergence problems. Therefore, the articular surfaces were moved apart during the model development and a clearance was given between the two surfaces. While running the analysis, a fixed displacement step equal to the amount of clearance previously specified between the two articular surfaces was imposed in the first step. This made the surfaces interact with each other and the loads were applied in the subsequent stages. This helped in solving the models with complex geometries and contact surfaces. Models like the patellofemoral cartilage having an overlap between the patella cartilage and femur cartilage were thus solved by separating the two surfaces initially. A displacement step was used in the first stage of the analysis to remove the contact gap modeled and get the contact between the two surfaces. The initial position of the patella before the start of the analysis was adjusted using the displacement control, i.e. the medial-lateral shift. It was aligned to a neutral position in the trochlear groove between the medial and lateral condyles. The tilt of the patella was also adjusted so that it does not have an uneven contact. The muscle forces were applied in the subsequent analysis stage.

3.8.2 Loading step

The deformed form of the model after the first stage of the analysis, the displacement step, served as the input for this stage. The finite element models of the patellofemoral joint had geometric non-linearity defined so that large deflections of the structures could be simulated. In this stage of the analysis, the quadriceps loads, as specified in the next section, were applied with the help of the linear springs representing the muscle bands VI, VL and VMO on the patella (Figure 3.23).

3.8.3 Output requests necessary for post processing

The data corresponding to the variables of interest (either kinematic or contact parameters) from the simulation model results were written to the output database of the ABAQUS/CAE by specifying ‘output requests’. The two types, i.e. field output requests and history output requests varied in the manner in which the data was requested from the models. While the field output requests for a variable were made for an entire region of the model or for particular portions of the model, the history output requests were made for variables from some specific points in the model. The data for the variables selected were obtained either at the end of the increment, after a set of time points or for a certain frequency specified for both the types.

For the present study, the stress and strain components in the region of interest, translations and rotations, reaction forces and contact parameters were obtained through the field output requests. The forces in the linear spring and wire elements and the contact area between the two articular cartilage structures

were measured after the analysis of the models with the help of history output requests.

3.9 Load module

The load module was for creating the boundary conditions and loading conditions. Boundary conditions were defined to specify the displacement and rotation of some bodies while restricting the others. Loading conditions were defined to apply the loads on the structures.

3.9.1 Boundary conditions

Boundary conditions were defined for the model to mimic the movement of the bones and cartilage structures at the patellofemoral joint during the flexion movement performed at the time of MRI scan procedure. As mentioned in previous sections, the femur and patella were defined as rigid bodies while the patella cartilage and femur cartilage were modeled as deformable bodies. For all the bodies modeled in the joint, ‘displacement / rotation’ boundary conditions were applied.

The femur in the patellofemoral joint was restrained motion throughout the analysis taking the global coordinate system as reference. This was done by specifying that it was not free to move in any of the six degrees of freedom at the femur rigid body reference point (FRP) (Figure 3.24).

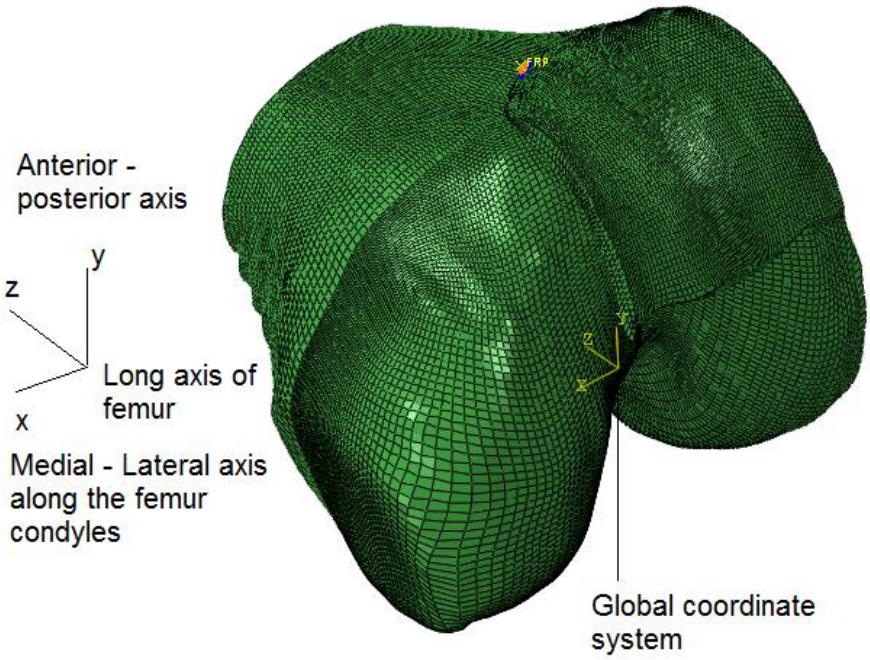

Figure 3.24: Boundary conditions for the femur bone applied at the point FRP (No motion in all six degrees of freedom).

The patella was allowed to move only to facilitate the patella cartilage to interact with the femur cartilage during the displacement step and it was given boundary conditions such that it had free motion in all six degrees of freedom in the loading step (Figure 3.25). The patella, along with the patella cartilage, was moved initially making way for a clearance while modeling the joint to avoid any overlap between the two cartilage structures. This same magnitude of motion was provided to the patella in the displacement step.

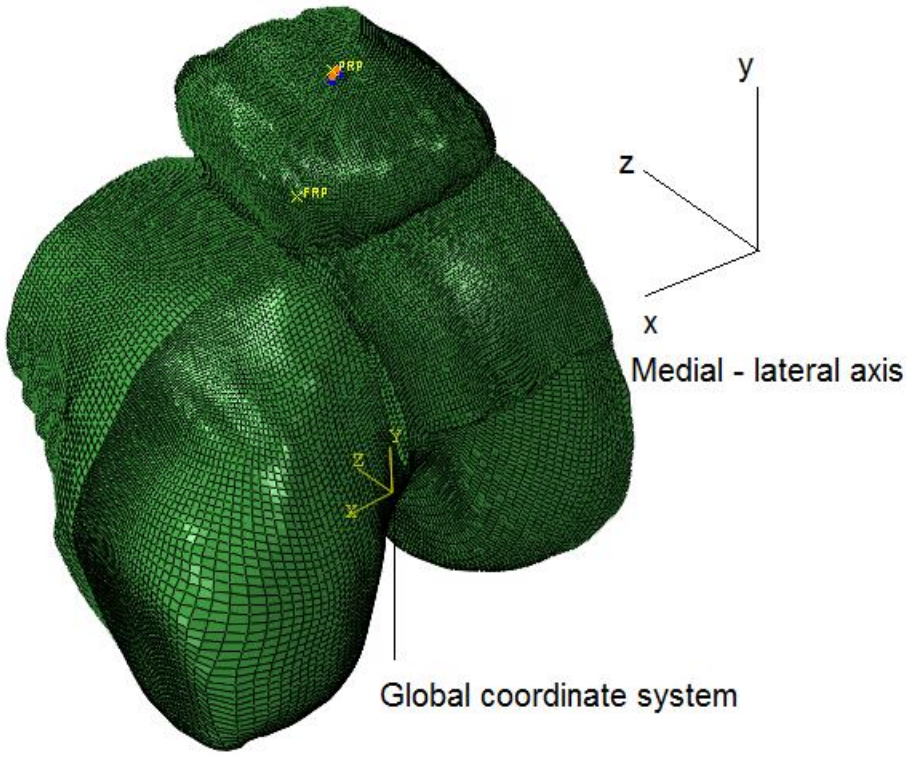

Figure 3.25: Boundary conditions for the patella bone applied at the point PRP.

With reference to the global coordinate system, the linear springs representing the patella tendon were given boundary conditions at its attachment points on the tibial tubercle, to restrict motion in all six degrees of freedom throughout the analysis. The boundary conditions for linear springs representing the quadriceps muscle bands VI, VL and VMO were defined with respect to the three datum coordinate systems VI_csys, VL_csys and VMO_csys, respectively (Figure 3.26). As mentioned previously in the assembly module section, these three datum coordinate systems were oriented with their X-axes directed towards the linear spring origin point on the shell planar plate from the patella insertion point. The motion in all six degrees of freedom was restricted for these spring elements in the displacement step. In the loading step, only the translational degrees of

freedom were allowed to move in the direction of applied load, i.e. only along the X-axis while the rotational degrees of freedom were restricted.

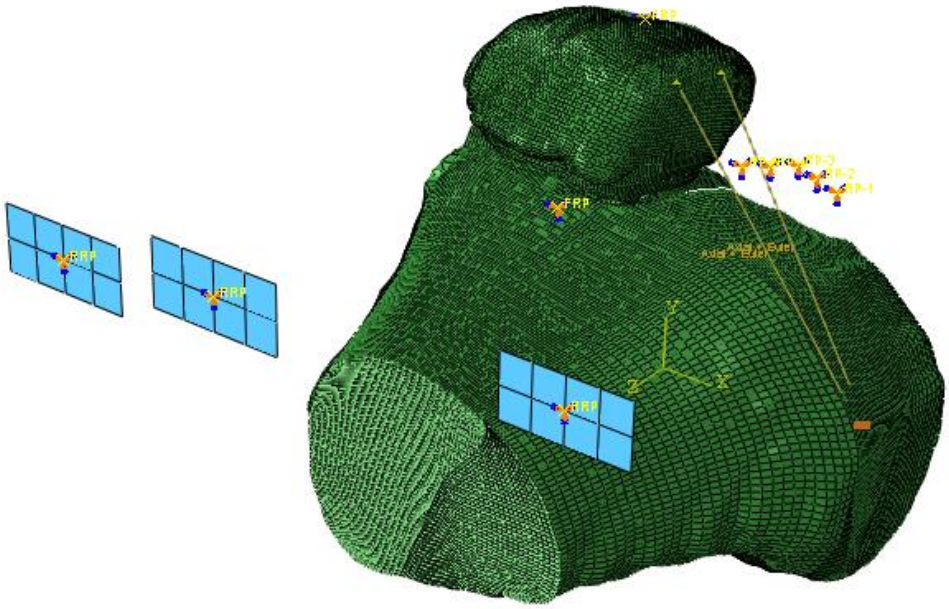

Figure 3.26: Boundary conditions for the patella tendon and quadriceps.

3.9.2 Loading conditions

Forces measured during the scan procedure were used to specify the loading conditions for the finite element model. Loading conditions were prescribed using the linear spring elements representing the quadriceps muscle bundles VI, VL and VMO. The loads were applied on the patella in the direction specified by the X-axis of the respective datum coordinate systems.

During the MRI scan procedure, the average force exerted by the patient using her foot on the foot plate was measured to be 70 N. This force on the foot plate was assumed to be balanced with the quadriceps moment at the knee joint. The

quadriceps moment arm was measured on the MRI scan taking a center of rotation of the knee joint at flexion angle 15°. The resulting quadriceps load was divided among the muscle bands VI, VL and VMO in the proportions of 74 %, 22 % and 4 %, respectively [24]. According to these divisions, the VI spring elements collectively had a load of 348.16 N, VL spring elements had a load of 102.35 N and the VMO spring elements had a load of 21.76 N (Figure 3.27). At all flexion angles, the forces applied through the quadriceps muscles had the same magnitudes.

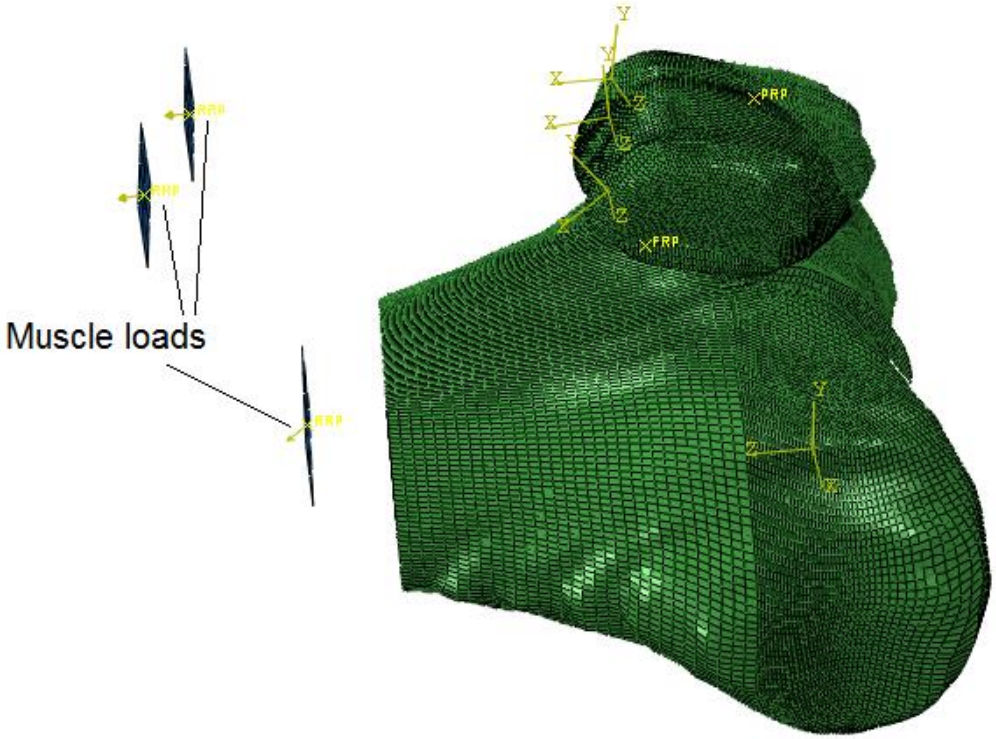

Figure 3.27: Loading conditions for the finite element model specified along the X-axes of the datum coordinate systems on rigid planar plates.

3.10 Mesh convergence analysis

Shah et al. (2012) developed patellofemoral joint models based on the similar modeling framework. Since the effects of the forces at the patellofemoral joint on the articular cartilage surface were the main concern for their model, a convergence analysis was performed for the number of hexahedral elements in the articular surfaces, i.e. the number of elements in the patella cartilage and the femur cartilage combined. The maximum contact pressure parameter versus the number of elements in the articular cartilages was used. It was observed in the study performed by Shah et al. (2012) that a minimum of 21,000 elements in the patella cartilage and femur cartilage combined, resulted in approximately a similar value of contact pressure. To speed up the modeling process for the present study, models were built based on this element number.

3.11 Data obtained from FE models

To measure the kinematics after the finite element simulations, anatomical landmark points were obtained from the models. The patellofemoral coordinate system, based on the joint coordinate system by Grood and Suntay (1983) was taken as the reference to measure the kinematics. Landmark points (most medial and lateral positions on the femur and patella, most distal position on patella and proximal points on femur) were taken from the results of the finite element models in both the pre-op and post-op simulations reflecting those that were digitized before the shape matching and meshing process of the structures. The rotations (flexion, valgus, external rotation) and translations (lateral, anterior,

distraction) were measured with the help of a floating axis patellofemoral coordinate system, which was described in Chapter 2.

At each flexion angle (15°, 19°, 22°, 36°, 49° and 57°), kinematics were obtained from the pre-op models and post-op models. A comparison was performed to examine whether there was any change in the lateral translation, lateral tilt and valgus with and without the presence of the MPFL graft elements. Validation of the patellofemoral joint finite element models was performed using these kinematic parameters. In addition, the tension in the ligament elements after the end of the analyses was obtained along with the ratio of tension between the patella tendon and the quadriceps muscle elements. The trends followed by these tension parameters with the change in flexion angle of the knee were examined with regard to the observations from previous in vitro studies

CHAPTER IV

RESULTS

4.1 Overview

This chapter provides a comparison between the kinematic results from the experimental MR imaging analysis and from the simulations of the patellofemoral joint finite element models for validation purposes. The trends followed by the ratios of tension in the patellar tendon to the quadriceps muscles (from the patellofemoral joint models with the MPFL graft and without the MPFL graft) and the variation of tension in the MPFL graft elements at the end of the analysis between the six different flexion angles were also included.

The kinematic parameters of the patella; lateral shift, lateral tilt, valgus and flexion were calculated using the joint coordinate system developed by Grood and Suntay (1983) as described in Chapter 2. Patellofemoral flexion was measured as the rotation of the patella about the transepicondylar (X) axis of the femur. External rotation (lateral tilt) was the rotation about the femoral long axis (Z-axis). Lateral shift was the translation measured along the transepicondylar axis with the medial direction being positive. Valgus was the external rotation of patella about the Y-axis.

4.2 Comparison between experimental and FEA kinematic results

The kinematic parameters were obtained from the finite element models and experimental imaging analysis performed for one subject. Lateral translation results from the experimental imaging analysis (Figure 4.1) and FEA analysis (Figure 4.2) were compared for validation.

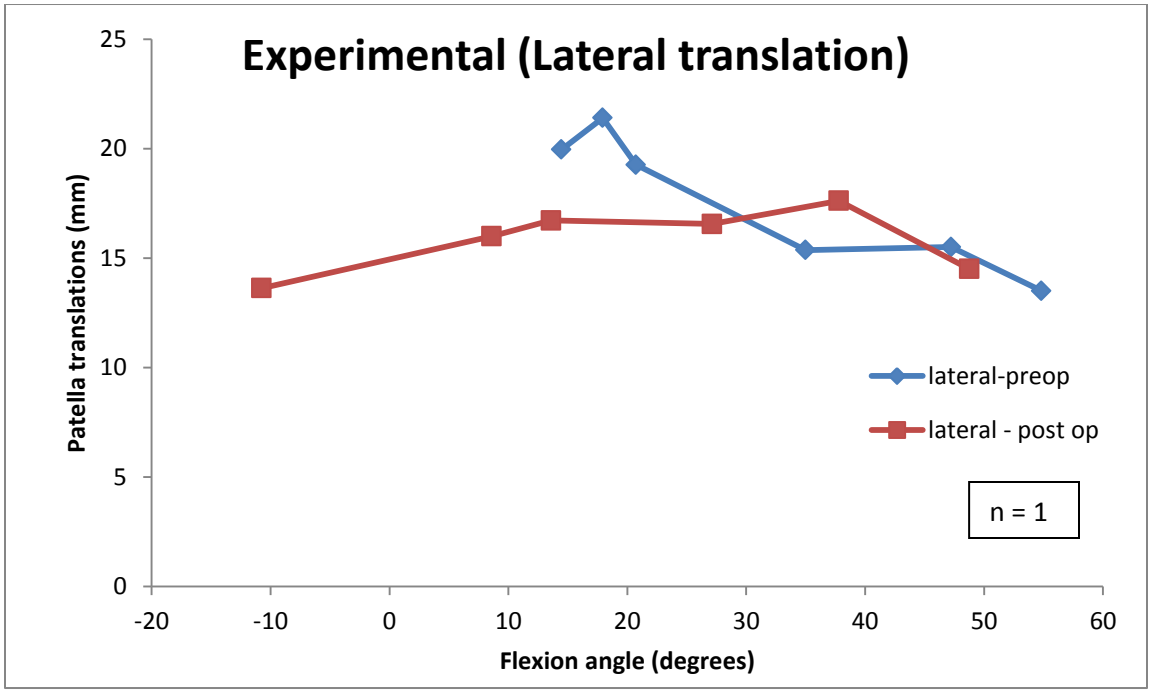

Figure 4.1: Lateral translation from experimental imaging analysis.

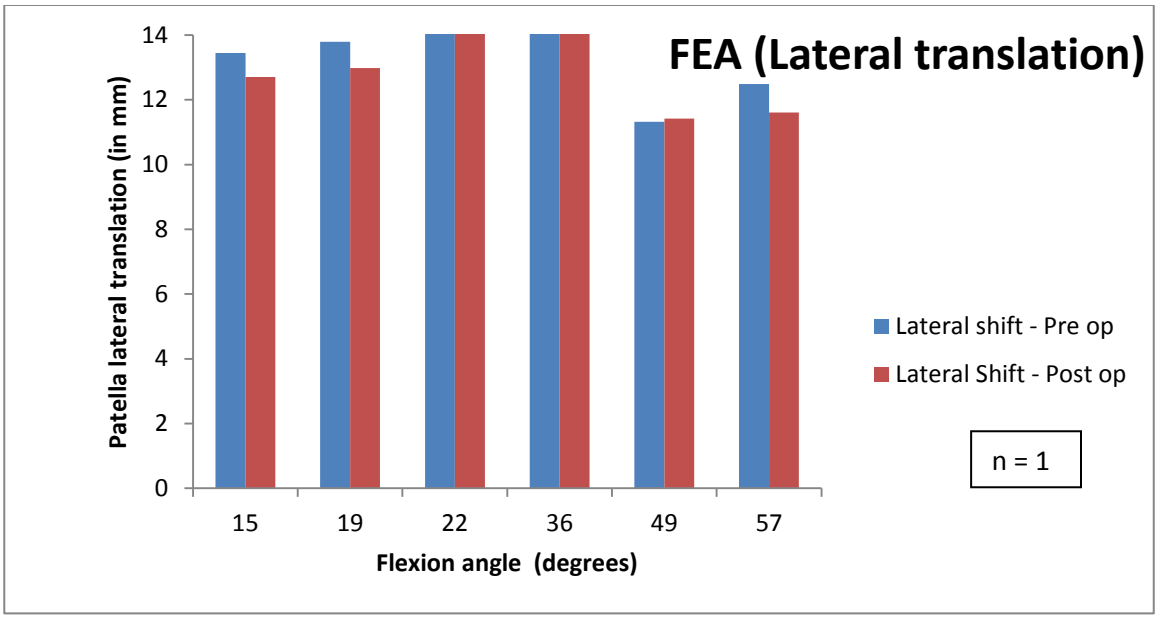

Figure 4.2: Lateral translation from FEA.

Lateral translation was observed to decrease in the post-op analysis and a similar trend was observed in FEA analysis and imaging analysis. The MPFL graft influenced shift of the patella joint at early flexion angles. For example, at angle of 15°, before the reconstruction of the ligament, a lateral translation of 19.96 mm was observed compared to 13.63 mm after replacing the ruptured ligament with the graft. The FEA analysis resulted in a lateral translation of 13.44 mm and 12.70 mm for the pre-op and post-op models, respectively.

The lateral tilt of the patella was used for validation. The MPFL graft had an influence on the tilt of the patella at early flexion angles. Results from experimental imaging analysis (Figure 4.3) and FEA analysis (Figure 4.4) showed a decrease in the tilt of the patella in the lateral direction at angles 15°-22°. At higher flexion angles 36°, 49° and 57°, the FEA results showed less difference between the pre-op and post-op models.

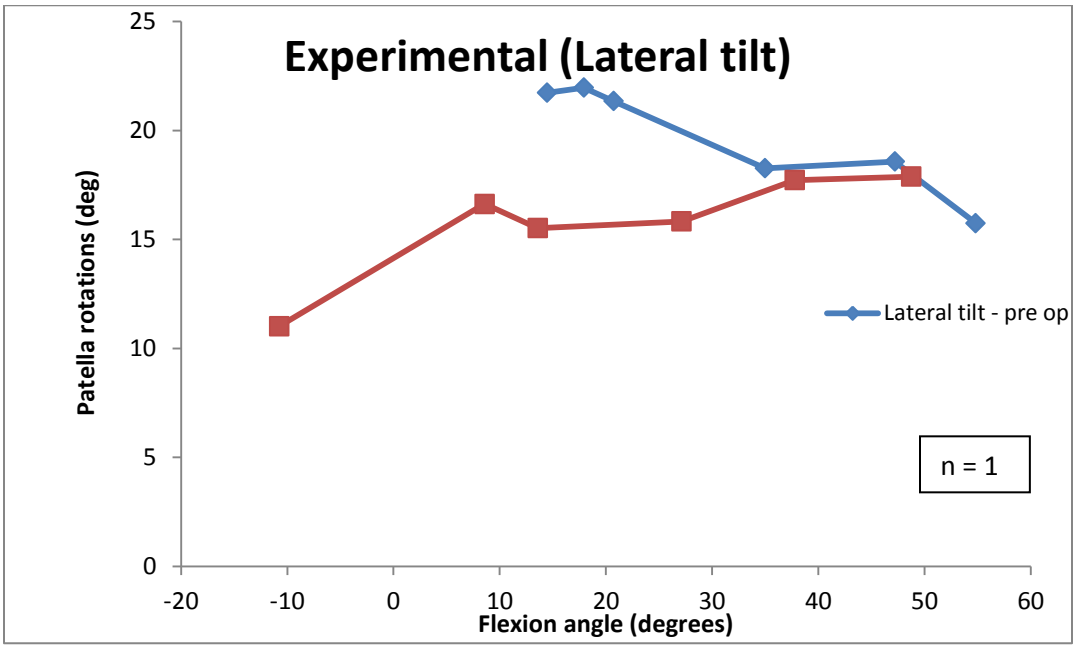

Figure 4.3: Lateral tilt from experimental imaging analysis.

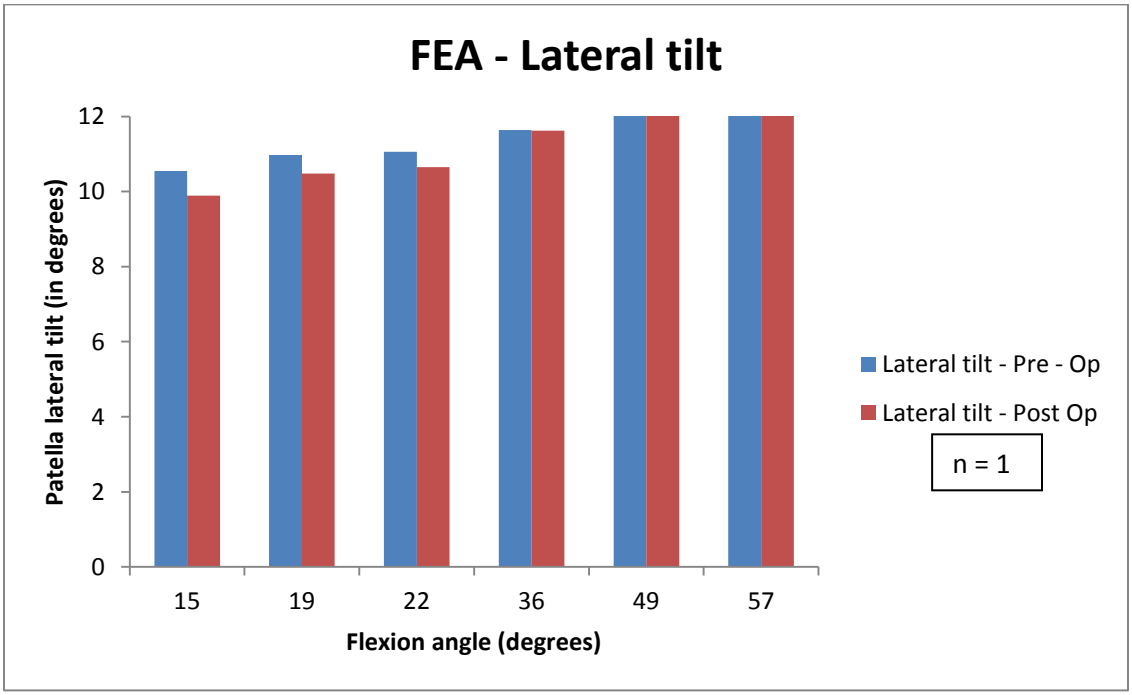

Figure 4.4: Lateral tilt from FEA.

Valgus rotation results from the experimental imaging analysis (Figure 4.5) and the FEA analysis (Figure 4.6) were also compared in addition to lateral translation and lateral tilt for validation. With the exception of the 15° angle, the valgus rotation also decreased in the FEA results (at 19° and 22°).

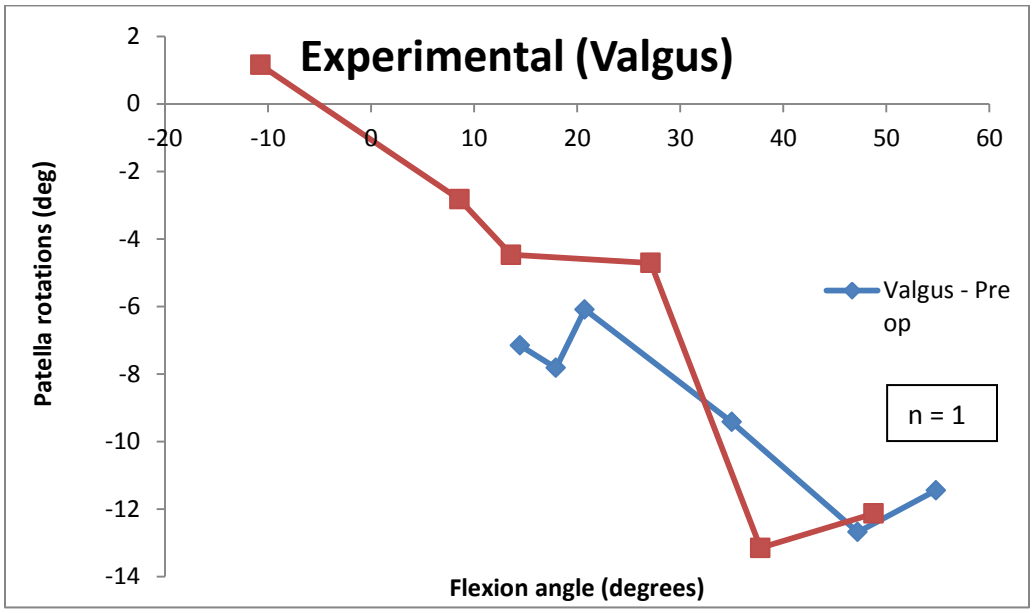

Figure 4.5: Valgus rotation from experimental imaging analysis.

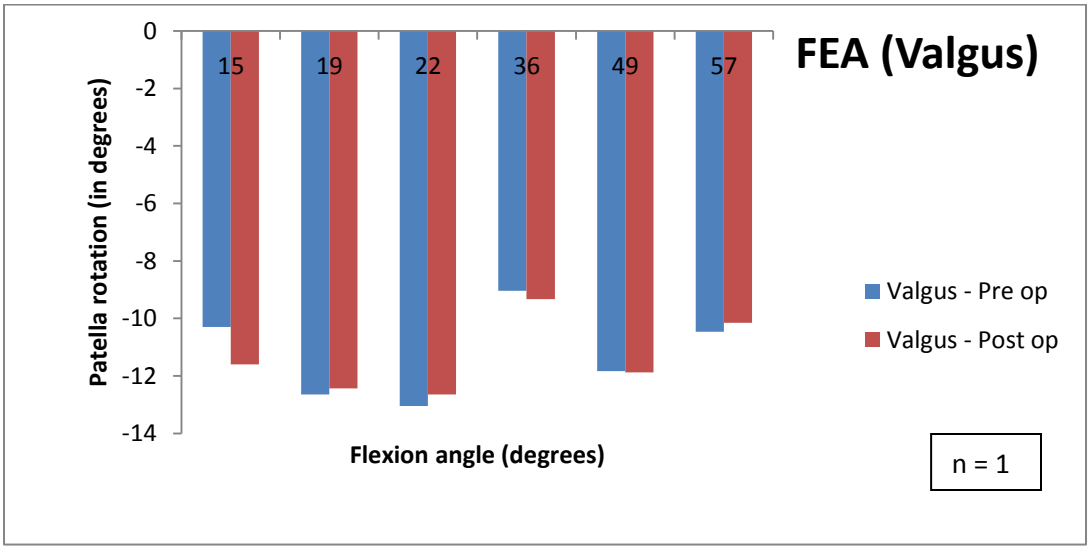

Figure 4.6: Valgus rotation from FEA.

The kinematic parameters from the experimental analyses were measured according to the shape matching procedures performed after reconstruction of the MRI data and alignment at different flexion angles. Though the results from the FE simulations replicated the trends followed by those from the experimental MRI analysis, they differed quantitatively.

4.3 Other kinematic parameters

The patellar flexion measured about the transepicondylar axis had similar values for both the models, with and without the MPFL graft elements. The patellar rotation increased as the flexion angle increased (Figure 4.7).

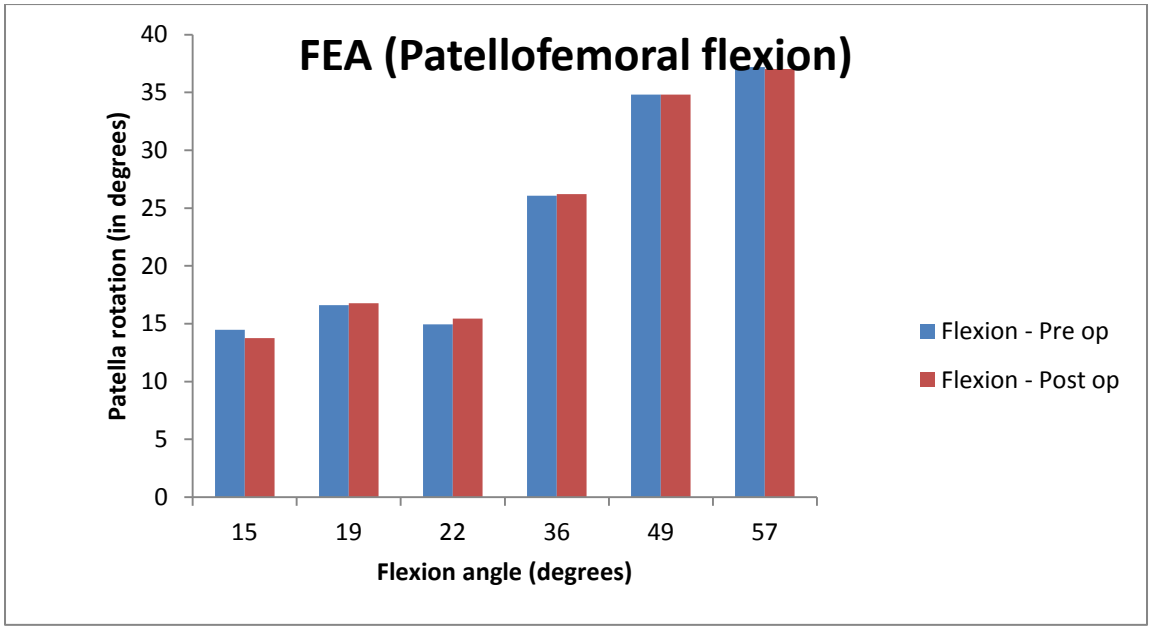

Figure 4.7: Patellofemoral flexion of pre-op and post-op from FEA.

4.4 Tensions in muscles and ligaments from finite element models

Linear tension only spring elements were used for representing the muscles. From the output of the finite element simulations, the tensions from the spring elements at the end of the analyses were taken and the ratio was calculated

between the tension in the patellar tendon and quadriceps muscle bands. The trend observed was similar between the models with and without the MPFL graft. The ratio between the tensions was higher at early flexion angles and it decreased to a value below 1 as the flexion angle increased (Figure 4.8).

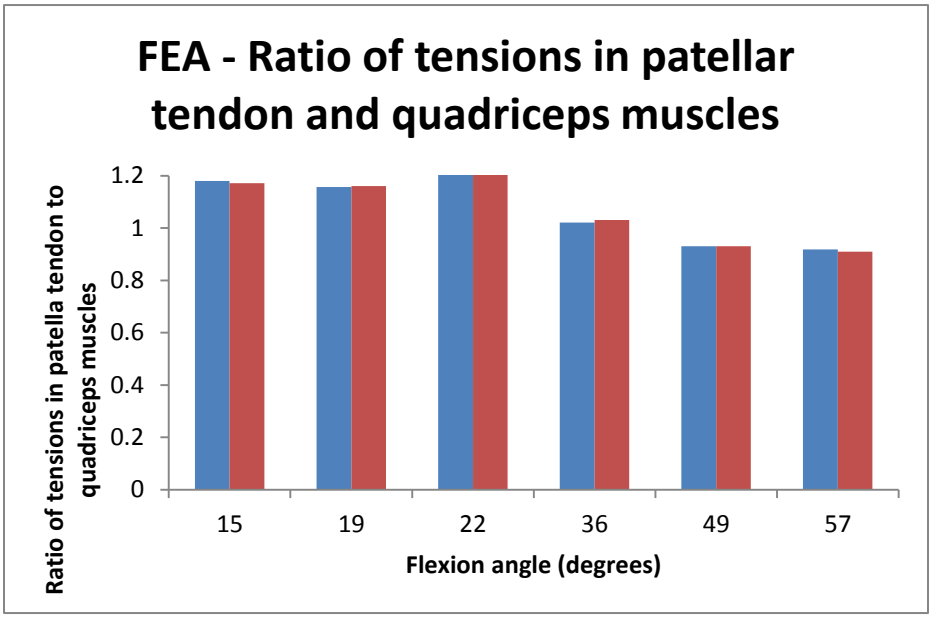

Figure 4.8: Ratio of tensions in patellar tendon and quadriceps muscles of pre-op and post-op from FEA.

The tension in the MPFL graft elements decreased to a value of 0 at a mid-flexion angle of 36° (Figure 4.9). At a flexion angle of 57°, the tension had a value of 18 N. This was thought to be due to the length change pattern in the uniaxial elements representing the MPFL graft and also the rotation and shift of the patella at 36°.

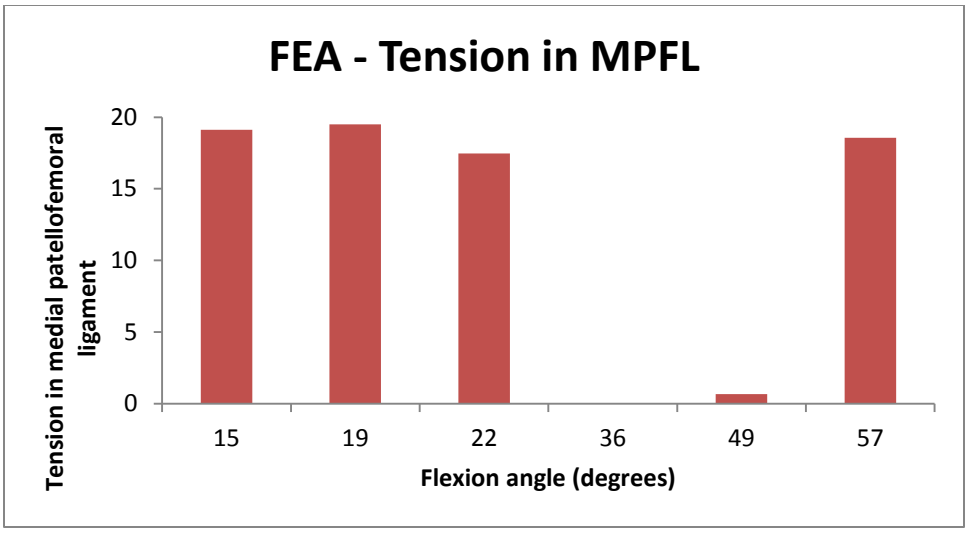

Figure 4.9: Tension in the MPFL graft elements corresponding to the six flexion angles from FEA.

CHAPTER V

DISCUSSION

5.1 Discussion

No previous study has been performed addressing the effects of the MPFL reconstruction exclusively on a symptomatic knee. The main objective of the present study was to mathematically develop a 3D subject specific finite element model to study the patellofemoral kinematics. Validation of these models was then performed with the results from MRI image analysis.

In the past, several in vitro studies have been performed using cadaver specimens to study the anatomy of the MPFL and the amount of resistance it offers to lateral tracking of the patella avoiding dislocation. An individual usually experiences patella dislocation at 20°-30° flexion [7, 10, 84]. Philippot et al. (2012), Conlan et al. (1993), Desio et al. (1998) and Hautamaa et al. (1998) have performed experiments to measure the percentage of the total lateral restraining force offered to the patella by the soft tissues on the medial aspect at these early flexion angles. They found that 50-60 % of the force was contributed by the MPFL and other medial retinaculum tissues contributed less. Bedi et al. (2010) found that the patella could be displaced laterally by 1 cm with a reduction in the force. In addition, studies also focused on the effects of the MPFL on

patellofemoral kinematics with intact and resected ligaments. Zaffagnini et al. (2013) and Ostermeier et al. (2007) measured the kinematics of the patellofemoral joint with and without the inclusion of the MPFL and found that the lack of the MPFL resulted in the possibility of the patella shifting laterally.

In vitro studies did not provide complete details such as the stresses and forces acting on the tissues or tension in the soft tissue ligaments, and they generally measured the change in kinematics with and without the presence of the MPFL. The in vivo kinematic behavior is difficult to measure and cannot be reproduced when performing experimental in vitro studies with non-physiological conditions. A quantitative measure of the kinematics and tension in the muscles and ligaments in vivo would provide a better insight into the behavior of the knee joint before and after undergoing an operative procedure. Computational models based on advanced numerical techniques provide a means of obtaining the patellofemoral kinematics. Finite element analysis is one such advanced numerical technique.

The main advantage that finite element modeling provides is that one can model the pathology related to the patellofemoral joint such as the patellar instability [92] and patellofemoral pain [67] using subject specific models. It allows the pressures and other forces acting on the tissues such as articular cartilage and ligaments to be calculated, while simulating their dynamic behavior in vivo. However, these models require validation. Computational models created exclusively for the knee joint were developed previously by various authors. Each addressed specific issues such as contact areas [42], joint stresses [67, 82],

biomechanics of the knee under various loading conditions to address tracking [51, 68], contact area and joint forces [86] and the effect of trochlear groove geometry on the joint stability [93]. Studies were also based on the modeling of the anterior cruciate and medial collateral ligaments [81, 83]. These models were validated using either kinematic or contact parameters. Validation is necessary so as to have an accurate measure of the forces present in vivo during dynamic movements of the knee joint and to extract related clinical information from these mathematical models.

In the current study, the subject had a MPFL deficiency along with a trochlear dysplasia. The MPFL reconstruction surgery was performed with a graft material from the semitendinosus tendon. MRI scans were taken before and after the reconstruction of the ligament. The subject did not exhibit any dislocation between the pre-op and post-op scans. Multi body 3D finite element models were built from the reconstructions of the scan data. It was observed that a hexahedral mesh of the articular surfaces provided a better mesh in the contact region as opposed to a tetrahedral mesh [74]. In addition, the hexahedral elements provided better regularity and higher accuracy, particularly for biomechanically complex soft tissue structures like articular cartilage [91]. As such, hexahedral meshes were developed for the patella and femoral articular cartilage structures, while surface meshes were built for the femur and patella.

The quadriceps muscle bands VI, VL and VMO and the patella tendon were modeled with linear tension only spring elements. Engelina S et al. (2012) studied the orientation angles of the VMO using a validated ultrasound

technique. They reported that lower orientation angles of the fibers of VMO muscle may affect the patella stability. Therefore, for the present study, the FE models were built with a low VMO orientation angle to accommodate for the weakness in the medial structures of the knee for this subject. In addition to the muscles and tendon, the MPFL ligament alone was modeled in the patellofemoral joint finite element models for this study to reduce complexity following the approach used in previous studies [81, 83]. Subject specific loads, measured during the MRI scan procedure were input to the finite element models. Boundary conditions were used to keep the femur fixed at all instances and the motion of the muscle bands was allowed along the direction of applied loads. Geometrical non-linearity was defined for the models so that the simulations accounted for the large deflections of the patella when loads were applied.

Digitized points were taken on the femur and patella for the calculation of kinematics using the joint coordinate system proposed by Grood and Suntay (1983). The kinematics obtained from the patellofemoral joint simulations produced similar trends as shown by the imaging analysis. The kinematics from the models without the MPFL graft elements failed to reflect those from the experimental analysis. The lateral translation and tilt did not reflect the experimental results quantitatively. However, they did support the observation that the presence of the MPFL reduced the lateral translation and tilt as depicted in the comparative plots in Chapter 4. A similar framework was used to model the patellofemoral joint with the anatomical geometry taken from the cadaver

specimens without any abnormalities by Shah et al. (2012). In their study, the pressure loading on the articular cartilage was studied by varying the patellofemoral loading and the models were validated with the contact and kinematic parameters from the in vitro studies. Kryshchuk et al. (2013) stated that there is a correlation between the actions of the MPFL and the severity of the trochlear dysplasia. The MPFL deficiency observed in conjunction with the trochlear dysplasia in the present subject was thought to influence the stability of the patella and also the kinematics in early knee flexion angles.

The ratio of the tensions in the patella tendon and quadriceps muscle bands varied between the models without the MPFL graft and the models with the MPFL graft. This ratio also varied as the flexion angle increased. These trends were similar to those observed in the in vitro studies conducted by Bishop et al. (1977), Ellis et al. (1980) and Huberti et al. (1984). Before applying the loads using the linear spring elements, for the patellofemoral joint model at a flexion angle of 15°, 40 N of tension was given to the MPFL graft elements (spring stiffness = 100 N/mm), to account for the graft tension. Measuring the length changes of these elements at subsequent angles (19°, 22°, 36°, 49° and 57°) helped in changing the graft tension values accordingly. At the end of the analysis, this tension was measured at different flexion angles and was found to decrease as the flexion angle was increased. As Bicos et al. (2007) predicted this was due to the loosening of the ligament as the patella entered the trochlear groove and the decrease in its role as a patella stabilizing component.

5.2 Limitations of the study

An acceptable simulation of the subject specific finite element models is largely dependent on the inputs used and assumptions made. The models were developed using an approximate modeling technique with valid assumptions to represent the in vivo behavior. The simulation of the models was influenced by the patient specific geometry, loading and boundary conditions and material properties of the tissues. To comprehend such simulations, valid assumptions were necessary regarding the parameters specified.

Geometrical problems were the main consideration. They arose due to manual tracing and reconstructing the structures while trying to obtain the knee geometry from the pre-op MRI scan data. It was necessary that we captured every small detail in the shape of the tissue being reconstructed and meshed to account for the contact areas. Even though it was small, the meshing process resulted in a loss of tissue shape features such as the sharp curves and unevenness in the reconstructed structures. A compromise was reached in some instances, regarding the mesh smoothing and quality of the elements while constructing the hexahedral mesh for complex structures such as the patella cartilage.

Normally, at the knee joint, due to interaction of several components, one observes complex physiologic loading patterns. Approximation is necessary to replicate this and so an estimate for the in vivo loads was taken. The quadriceps extension moment arm of the knee was measured from the MRI about the center of rotation of the knee. The subject specific foot load measured during the MRI scan was then used to calculate the quadriceps muscle load. As such, the

magnitude of the muscle load was dependent on the manually measured moment arm and the estimation.

To reduce the computational time and create an efficient analysis, the femur and patella were considered to be rigid bodies. A large sample study was conducted by Fitzpatrick et al. (2010) in which rigid and deformable subject specific finite element models were built to study the patellofemoral kinematics and contact mechanics. They looked at the computational analysis time and accuracy of the results. The kinematic parameters from the rigid and deformable body analyses were in good agreement and the root mean square differences were on the order of 0.5 deg. and 0.2 mm. Based on these results, they reported that there was 95 % reduction in computational time with rigid body models. In the present study, the bones were modeled as rigid structures to lower the computational time.

To model the dynamic behavior of tissues in vivo required that appropriate material properties were used. The present study used compromised material properties of the tissues (i.e. the Young's Modulus of the articular cartilage) due to finite element model convergence issues. To account for the short duration of the compressive loading of the cartilage during the low resolution MRI scans, it was initially modeled with lower values of Young's Modulus [94]. The finite element model at one of the flexion angles (36°) failed to achieve an equilibrium state upon the application of forces. This was corrected by increasing the Young's Modulus to a well-accepted value of 10 MPa [37, 38].

Muscle and ligament reconstruction from the patient MRI data was not possible due to the low resolution of the MRI scans at various flexion angles. Geometrical representation of the structures involved at the patellofemoral joint based on their anatomical features may have provided better insight into the joint behavior.

Normally, the lateral trochlea of the femur is at a higher and elevated position when compared to the medial trochlea and this in turn helps in restraining the patella from moving laterally. This was not seen for the knee of the subject in this study. Trochlear dysplasia was observed for the present subject with 0 mm depth of the trochlear groove on the anterior aspect of the distal femur. This trochlear dysplasia produced a high lateral translation in the pre-op models when compared to the post-op models of experimental imaging analysis [23, 25]. This was not evident in the finite element simulations due to model instability issues, though there was a difference between the kinematics of the pre-op and post-op models. Modeling issues of the patellofemoral joint such as contact initiations and initial tilt and shift restricted the patella translations and rotations. Due to this reason, the difference between the pre-op and post-op kinematic values from FEA simulations was not as large as those measured in the subject.

Only one subject was considered for the present study. Including additional subjects would have resulted in better observations and helped the validation of the finite element results with those of the experimental analysis.

5.3 Conclusion

Subject specific computational models were developed based on the 3D anatomical geometry obtained from the pre-op MRI data with valid assumptions. The models in the present study included the femur and patella along with their respective cartilage geometries. Though the kinematics of the patellofemoral joint finite element models had similar trends, they could not replicate the experimental MRI analysis results quantitatively and the validation was not successful. However, a decrease in the lateral translation and tilt was observed in the post-op models. Based on this observation, we can infer that the stability of the patellofemoral joint is governed by the soft tissues of the joint in addition to the bony geometry. The presence of the MPFL graft in the finite element models of the symptomatic patellofemoral joint proved that it is necessary and important for the stability of the patella. In addition, the ratio of tension in the patellar tendon and quadriceps muscles and the tension in the MPFL graft elements at the end of the simulations followed similar trends as reported in the literature.

5.4 Future work

The inputs given to the finite element models governed their behavior in every case. The models could be improved by:

i. Providing appropriate anatomical geometry for the ligaments and muscles along with their material properties.
ii. Ensuring that anatomical features are not lost while developing the finite element meshes for the structures.

iii. Developing finer meshes for the structures where contact is expected to occur so that there is accuracy while processing the results and validating them.

Performing a ligament reconstruction surgery with a graft material requires consideration of several factors. The technique used in this pilot study can be further applied to account for the inter subject differences. The anatomical geometry varies from subject to subject. This will have an effect on the patellofemoral joint finite element models. For the subject population that includes pediatrics and young athletes, the growth plate is open at the femur condyles. Finite element models can be used to study the varying attachment points on the femur and patella so that the surgeons do not interfere with the growth plates while performing a ligament reconstruction surgery. The necessary graft tensioning required at a particular flexion angle of the knee while performing the surgery can also be studied. This tensioning is needed so that the reconstructed graft performs the function of the natural ligament at 20°-30° flexion angles. In addition, simulation of other surgical techniques such as tibial tubercle transfer can be studied.

REFERENCES

1. Gray, Henry. Anatomy of the Human Body. Philadelphia: Lea & Febiger, 1918; Bartleby.com, 2000.

2. Ewing JW (ed): Articular cartilage and knee joint function. New York, Raven, 1990.

3. Dye SF. Patellofemoral anatomy. In: Fox JM, Del Pizzo W. eds. The Patellofemoral joint. New York: McGraw-Hill Inc. 1993.

4. Meachim G: Cartilage lesions of the patella, in: Pickett JC, Radin EL (eds): Chondromalacia of the Patella. Baltimore, Williams & Wilkins, 1983.

5. Cofield RH and Bryan RS: Acute dislocation of the patella: Results of conservative treatment. *J Trauma.* 1977*;* 17: 526-31.

6. Fithian DC, Paxton EW, Stone ML, Silva P, Davis DK, Elias DA, White LM: Epidemiology and natural history of acute patella dislocation*. Am J Sports Med.* 2004; 32(5): 1114-21.

7. Hungerford DS, Barry M. Biomechanics of the patellofemoral joint. *Clin Orthop Relat* Res. 1979; 144 (8): 9-15.

8. Besl PJ, McKay Neil D. A method for registration of 3-D shapes. Pattern Analysis and Machine Intelligence*. IEEE Trans. On Pattern Analysis and Machine Intelligence*. 1992; 14(2): 239—256.

9. Herbert Kaufer. Mechanical Function of the Patella. *J Bone Joint Surg Am*. 1971; 53 (8): 1551-1560.

10. Amis AA, Firer P, Mountney J, Senavongse W, Thomas NP. Anatomy and biomechanics of the medial patellofemoral ligament. *The Knee*. 2003; *10*(3): 215–20.

11. Tuxøe JI, Teir M, Winge S, Nielsen PL. The medial patellofemoral ligament : a dissection study*. Knee Surg Sports Traumatol Arthrosc.* 2002; 10(3): 138–140.

12. Smirk C, Morris H. The anatomy and reconstruction of the medial patellofemoral ligament*. Knee*. 2003; 10: 221–227.

13. Dath R, Chakravarthy J, Porter K. Patella dislocations. *Trauma*. 2006; 8(1): 5–11.

14. LaPrade RF, Engebretsen AH, Ly TV, Johansen S, Wentorf FA, Engebretsen L. The anatomy of the medial part of the knee. *J Bone Joint Surg Am*. 2007; 89(9): 2000-10.

15. Noyes FR, Albright JC. Reconstruction of the medial patellofemoral ligament with autologous quadriceps tendon. *Arthroscopy*. 2006; 22: 904.e1 – 904.e7.

16. Nomura E. Cartilage Lesions of the Patella in Recurrent Patellar Dislocation. *Am J Sports Med*. 2004; *32*(2): 498–502.

17. Baldwin JL. The Anatomy of the Medial Patellofemoral Ligament. *Am J Sports Med*. 2009; 37(12): 2355–2361.

18. Warren LF, Marshall JL. The supporting structures on the medial side of the knee: an anatomical analysis*. J Bone Joint Surg Am*. 1979; 61(1): 56-62.

19. Sallay PI, Poggi J, Speer KP, Garrett WE. Acute dislocation of the patella. A correlative pathoanatomic study. *Am J Sports Med.* 1996; 24(1): 52-60.

20. Nomura, E. Classification of lesions of the medial patello-femoral ligament in patellar dislocation. *International orthopaedics*. 1999; *23*(5): 260–3.

21. Conlan T, Garth WP, Lemons JE. Evaluation of the medial soft-tissue restraints of the extensor mechanism of the knee. *J Bone Joint Surg Am*. 1993; *75*(5): 682–93.

22. Desio SM, Burks RT, Bachus KN. Soft tissue restraints to lateral patellar translation in the human knee. *Am J Sports Med*. 1998; *26*(1): 59–65.

23. Feller JA, Amis AA, Andrish JT, Arendt EA, Erasmus PJ, Powers CM. Surgical biomechanics of the patellofemoral joint. *Arthroscopy*. 2007; 23(5): 542-53.

24. Kushal Shah: The influence of hamstring loading on patellofemoral biomechanics: A finite element study. May 2012.

25. Hao Feng: The computational reconstruction and evaluation of the patellofemoral instability. May 2013.

26. Hautamaa PV, Fithian DC, Kaufman KR, Daniel DM, Pohlmeyer AM. Medial Soft tissue restraints in lateral patellar instability and repair. *Clin Orthop Relat Res.* 1998, 4(349): 174-82.

27. Liu XL, Mow VC. Biomechanics of articular cartilage and determination of material properties. *Med Sci Sports Exerc.* 2008; 40(2): 193-199.

28. Reider B, Marshall DVM, Koslin B, Ring B, Girgis FG. The anterior aspect of the knee joint. *J Bone Joint Surg Am*. 1981; 63: 351-356.

29. Powers CM, Ward SR, Chan LD, Chen YJ, Terk MR. The effect of bracing on patella alignment and patellofemoral joint contact area*. Med Sci Sports Exerc.* 2004; 36(7): 1226-32.

30. Neil Upadhyay, Charles Wakeley, Jonathan D.J. Eldridge. Patellofemoral instability. *Orthopaedics and Trauma*. 2010; 24(2): 139 – 148.

31. Colvin AC, West RV. Patellar instability. *J Bone Joint Surg Am.* 2008; 90(12): 2751-62.

32. Smith TO, Walker J, Russell N. Outcomes of medial patellofemoral ligament reconstruction for patellar instability: a systematic review. *Knee Surg Sports Traumatol Arthrosc*. 2007; 15(11): 1301-14.

33. Buckens CFM, Saris DBF. Reconstruction of the medial patellofemoral ligament for treatment of patellofemoral instability: A systematic review. *Am J Sports Med.* 2010; 38(1): 181-188.

34. Ellera Gomes, J. L. Medial patellofemoral ligament reconstruction for recurrent dislocation of the patella: a preliminary report. *Arthroscopy.* 1992; *8*(3): 335–40.

35. Ellera Gomes JL, Stigler Marczyk LR, Cesar de Cesar P, Jungblut CF. Medial patellofemoral ligament reconstruction with semitendinosus autograft for chronic patellar instability: a follow up study. Arthroscopy. 2004; 20(2): 147-51.

36. Waterman BR, Belmont PJ Jr, Owens BD. Patellar dislocations in the United States: role of sex, age, race, and athletic participation. *J Knee Surg.* 2012; 25(1): 51-7.

37. Fernandez JW, Hunter PJ, Shim V, Mithraratne P. A Subject specific framework to inform musculoskeletal modeling: Outcomes from the IUPS physiome project. *Patient Specific Computational Modeling.* 2012; 39–60.

38. Blankevoort L, Kuiper JH, Huiskes R, Grootenboer HJ. Articular contact in a three-dimensional model of the knee. *Journal of biomechanics*. 1991; *24*(11): 1019–31.

39. TrueGrid, User's Manual, Volume 1, Version 2.3.0, April 6, 2006.

40. Abaqus Analysis User's Manual, Abaqus 6.12 Documentation collection.

41. Besier TF, Gold GE, Beaupr GS, Delp SL. A Modeling Framework to Estimate Patellofemoral Joint Cartilage Stress In Vivo. *Medicine & Science in Sports & Exercise*. 2005; *37*(11): 1924–30.

42. Besier TF, Draper CE, Gold GE, Beaupré GS, Delp SL. Patellofemoral joint contact area increases with knee flexion and weight-bearing. *Journal of orthopaedic research : official publication of the Orthopaedic Research Society*. 2005; *23*(2): 345–50.

43. Parikh SN, Nathan ST, Wall EJ, Eismann EA. Complications of medial patellofemoral ligament reconstruction in young patients. *Am J Sports Med.* 2013; *41*(5): 1030–8.

44. Philippot R, Boyer B, Testa R, Farizon F, Moyen B. The role of the medial ligamentous structures on patellar tracking during knee flexion. *Knee Surg Sports Traumatol Arthrosc*. 2012; 20(2): 331–6.

45. Yoo YS, Chang HG, Seo YJ, Byun JC, Lee GK, Im H, Song SY. Changes in the length of the medial patellofemoral ligament: an in-vivo analysis using 3-dimensional computed tomography. *Am J Sports Med*. 2012; 40(9): 2142-8.

46. Stephen JM, Lumpaopong P, Deehan DJ, Kader D, Amis AA. The medial patellofemoral ligament: location of femoral attachment and length change patterns resulting from anatomic and non-anatomic attachments. *Am J Sports Med*. 2012; 40(8): 1871-9.

47. Servien E, Fritsch B, Lustig S, Demey G, Debarge R, Lapra C, Neyret P. In vivo positioning analysis of medial patellofemoral ligament reconstruction. *Am J Sports Med*. 2011; 39(11): 134-9.

48. Steensen RN, Dopirak RM, McDonald WG 3rd. The Anatomy and Isometry of the Medial Patellofemoral Ligament Implications for Reconstruction. *Am J Sports Med.* 2004; 32(6): 1509–13.

49. Ahmad CS, Stein BE, Matuz D, Henry JH. Immediate surgical repair of the medial patellar stabilizers for acute patellar dislocation. *Am J Sports Med.* 2000; 28(6): 804-10.

50. Andrish J. The management of recurrent patellar dislocation. *The Orthopedic clinics of North America*. 2008; *39*(3): 313–27.

51. Fitzpatrick CK, Baldwin MA, Rullkoetter PJ. Computationally efficient finite element evaluation of natural patellofemoral mechanics. J Biomech Eng. 2010; 132 (12): 1210-13.

52. FItzpatrick CK, Rullkoetter PJ. Influence of patellofemoral articular geometry and material on mechanics of the unresurfaced patella. J Biomech. 2012; 45(11): 1909-15.

53. Siebold R, Chikale S, Sartory N, Hariri N, Feil S, Passler HH. Hamstring graft fixation in MPFL reconstruction at the patella using a transosseous suture technique. *Knee Surg Sports Traumatol Arthrosc.* 2010; 18(11): 1542-4.

54. Bedi H, Marzo J. The biomechanics of medial patellofemoral ligament repair followed by lateral retinacular release. *Am J Sports Med.* 2010; *38*(7): 1462–7.

55. Beillas P, Papaioannou G, Tashman S, Yang KH. A new method to investigate in vivo knee behavior using a finite element model of the lower limb. *Journal of biomechanics*. 2004; *37*(7): 1019–30.

56. Nomura EU, Horiuchi Y, Kihara M. Medial patellofemoral ligament restraint in lateral patellar translation and reconstruction. *Knee*. 2000; 7(2): 1–7.

57. Tanaka MJ, Bollier MJ, Andrish JT, Fulkerson JP, Cosgarea AJ. Complications of medial patellofemoral ligament reconstruction: common technical errors and factors for success: AAOS exhibit selection. *The Journal of bone and joint surgery. American volume*. 2012; *94*(12): e87.

58. Zaffagnini S, Colle F, Lopomo N, Sharma B, Bignozzi S, Dejour D, Marcacci M. The influence of medial patellofemoral ligament on patellofemoral joint kinematics and patellar stability. *Knee surgery, sports traumatology, arthroscopy : official journal of the ESSKA*. 2013; *21*(9): 2164–71.

59. Beck P, Brown NA, Greis PE, Burks RT. Patellofemoral Contact Pressures and Lateral Patellar Translation after Medial Patellofemoral Ligament Reconstruction. *Am J Sports Med.* 2007; 35(9): 1557–63.

60. Elias JJ, Cosgarea AJ. Atlas of the Patellofemoral Joint. (V. Sanchis-Alfonso, Ed.). 2013; 135–8.

61. Elias JJ, Cosgarea AJ. Anterior knee pain and patellar instability. (V. Sanchis-Alfonso, Ed. 2011; 287–297.

62. Elias JJ, Kirkpatrick MS, Saranathan A, Mani S, Smith LG, Tanaka MJ. Hamstrings loading contributes to lateral patellofemoral malalignment and elevated cartilage pressures : An in vitro study. *Clin Biomech*. 2011; *26*(8), 841–6.

63. Elias JJ, Coasgarea AJ. Technical errors during medial patellofemoral ligament reconstruction could overload medial patellofemoral cartilage: a computational analysis. *Am J Sports Med.* 2006; 34(9): 1478-85.

64. Ohman C, Espino DM, Heinmann T, Baleani M, Delingette H, Viceconti M. Subject-specific knee joint model: Design of an experiment to validate a multi-body finite element model. The visual computer (2011); 27(2):153-9.

65. Van de Velde SK, Gill TJ, Li G. Dual fluoroscopic analysis of the posterior cruciate ligament - deficient patellofemoral joint during lunge. *Med Sci Sports Exerc*. 2009; 41(6): 1198-205.

66. Viceconti M, Olsen S, Nolte LP, Burton K. Extracting clinically relevant data from finite element simulations. *Clinical biomechanics (Bristol, Avon)*. 2005; *20*(5): 451–4.

67. Farrokhi S, Keyak JH, Powers C M. Individuals with patellofemoral pain exhibit greater patellofemoral joint stress: a finite element analysis study. *Osteoarthritis and cartilage / OARS, Osteoarthritis Research Society*. 2011; *19*(3): 287–94.

68. Mesfar W, Shirazi-Adl A. Biomechanics of the knee joint in flexion under various quadriceps forces. *The Knee*. 2005; *12*(6): 424–34.

69. Huberti HH, Hayes WC, Stone JL, Shybut GT. Force ratios in the quadriceps tendon and ligamentum patellae. *Journal of orthopaedic research : official publication of the Orthopaedic Research Society*. 1984.

70. Hefzy MS, Yang H. A three-dimensional anatomical model of the human patello-femoral joint, for the determination of patello-femoral motions and contact characteristics. *Journal of biomedical engineering*. 1993; *15*(4): 289–302.

71. Grood ES, Suntay WJ. A joint coordinate system for the clinical description of three-dimensional motions: application to the knee. *Journal of biomechanical engineering*. 1983; *105*(2): 136–44.

72. Bicos J, Fulkerson JP, Amis, A. Current concepts review: the medial patellofemoral ligament. *Am J Sports Med*. 2007; *35*(3): 484–92.

73. Stäubli HU, Schatzmann L, Brunner P, Rincón L, Nolte LP. Quadriceps tendon and patellar ligament: cryosectional anatomy and structural properties in young adults. *Knee Surg Sports Traumatol Arthrosc*. 1996; *4*(2): 100–10.

74. Ramos A, Simoes JA. Tetrahedral versus hexahedral finite elements in numerical modeling of the proximal femur. *Med Eng Phys*. 2006; 28(9): 916-24.

75. Engelina S, Roberson CJ, Moggridge J, Killingback A, Adds P. Using ultrasound to measure the fibre angle of vastus medialis obliqus: A cadaveric study. *Knee.* 2012.

76. Bishop RED, Denham RA. A note on the ratio between tensions in the quadriceps tendon and infra-patellar ligament. *Engineering in Medicine*. 1977; 6: 53.

77. Ellis MI, Seedhom BB, Wright V, Dowson D. An evaluation of the ration between the tensions along the quadriceps tendon and patellar ligament. *Engineering in Medicine*. 1980; 9:189.

78. Huberti HH, Hayes WC, Stone JL, Shybut GT. Force ratios in the quadriceps tendon and ligamentum patellae. *J Orthop Res.* 1984; 2(1): 49-54.

79. Bitar AC, Demange MK, D'Elia CO, Camanho GL. Traumatic patellar dislocation: Non operative treatment compared with MPFL reconstruction using patellar tendon. *Am J Sports Med.* 2012; 40(1): 114-122.

80. Feller JA, Feagin JA, Garret Jr. WE. The medial patellofemoral ligament revisited: an anatomical study. *Knee Surg Sports Traumatol Arthrosc*.1993; 1: 184-6.

81. Gardiner JC, Weiss JA. Subject specific finite element analysis of the human medial collateral ligament during valgus knee loading. *J Orthop Res*. 2003; 21(6): 1098-106.

82. Besier TF, Gold GE, Delp SL, Fredericson M, Beaupre GS. The influence of femoral internal and external rotation on cartilage stresses within the patellofemoral joint*. J Orthop Res*. 2008; 26(12): 1627-35.

83. Limbert G, Taylor M, Middleton J. Three dimensional finite element modeling of the human ACL: simulation of passive knee flexion with a stressed and stress-free ACL*. J Biomech*. 2004; 37(11): 1723-31.

84. Senavongse W, Amis AA. The effects of articular, retinacular or muscular deficiencies on patellofemoral joint stability: a biomechanical study in vitro. *J Bone Joint Surg Br.* 2005; B7: 577-582.

85. Ostermeier S, Holst M, Bohnsack M, Hurschler C, Stukenborg-Colsman C, Wirth CJ. In vitro measurement of patellar kinematics following reconstruction of the medial patellofemoral ligament. *Knee Surg Sports Traumatol Arthrosc.* 2007; 15(3): 276-85.

86. Akbar M, Farahmand F, Jafari A, Foumani MS. A detailed and validated three dimensional dynamic model of the patellofemoral joint. *J Biomech Eng*. 2012; 134(4): 041005.

87. Ciccone WJ II, Bratton DR, Weinstein DM, Elias JJ. Viscoelasticity and temperature variations decrease tension and stiffness of hamstring tendon grafts following anterior cruciate ligament reconstruction*. J Bone Joint Surg Am*. 2006; 88(5): 1071-8.

88. Nelitz M, Dreyhaupt J, Reichel H, Woelfle J, Lippacher S. Anatomic reconstruction of the medial patellofemoral ligament in children and adolescents with open growth plates: surgical technique and clinical outcome. *Am J Sports Med*. 2013; 41(1): 58-63.

89. Thaunat M, Erasmus PJ. Recurrent patellar dislocation after medial patellofemoral ligament reconstruction. *Knee Surg Sports Traumatol Arthrosc*. 2008; 16(1): 40-3.

90. Schottle PB, Schmeling A, Rosenstiel N, Weiler A. Radiographic landmarks for femoral tunnel placement in medial patellofemoral ligament reconstruction. *Am J Sports Med.* 2007; 35(5): 801-4.

91. Cifuentes AO, Kalbag A. A performance study of tetrahedral and hexahedral elements in 3 - D finite element structural analysis. *Finite Elem Anal Des.* 1992; 12(3-4): 313-8.

92. Kryshchuk M., Buryanov A, Lykhodii V., Ieshchenko V. Computer modeling of patellar instability in association with trochlear dysplasia. Journal of Mechanical Engineering NTUU. 2013.

93. Jafari A, Farahmand F, Meghdari A. The effects of trochlear groove geometry on patellofemoral joint stability – a computer model study. *Proc Inst Mech Eng H.* 2008; 222(1): 75-88.

94. Shepherd D.E.T and Seedhom B.B. A technique for measuring the compressive modulus of articular cartilage under physiological loading rates with preliminary results. *Journal of Engineering in Medicine*. 1997; 211: 155-165.

95. Staubli HU, Schatzmann L. Quadriceps tendon and patellar ligament: cryosectional anatomy and structural properties in young adults. *Knee Surg Sports Traumatol Arthrosc.* 1996; 4(2): 100-10.

96. Delp SL, Loan JP. A graphics based software system to develop and analyze models of musculoskeletal structures. *Comput Biol Med*. 1995; 25(1): 21-34.

97. Philippot R, Boyer B, Testa R, Farizon F, Moyen B. Study of patellar kinematics after reconstruction of the medial patellofemoral ligament. *Clin Biomech (Bristol, Avon).* 2012; 27(1): 22-6.

98. Archana Saranathan. In vitro characterization of the influence of tibial tuberosity transfers on patellofemoral pressures with and without patellar cartilage lesions. August 2010.

APPENDICES

APPENDIX A

INPUT FILE FOR ABAQUS

```
**Knee BC15 input file
**=====================================================
*PART, NAME=Femur
*INCLUDE, INPUT=femur
** Section:
*SHELL GENERAL SECTION, MATERIAL=M1, ELSET=SS1M1,
ORIENTATION=COR1
0.0
,
*END PART
**=====================================================
*PART, NAME=Femur Cartilage
*INCLUDE, INPUT=femcart
** Section:
*SOLID SECTION, ELSET=PM1, MATERIAL=unknown, ORIENTATION=SOR1
,
*END PART
**=====================================================
*PART, NAME=Patella
```

*INCLUDE, INPUT=patella_15

** Section:

*SHELL GENERAL SECTION, MATERIAL=M1, ELSET=SS1M1,
ORIENTATION=COR1

0.0

,

*END PART

**===

*PART, NAME=Patella Cartilage

*INCLUDE, INPUT=patcart_15

** Section:

*SHELL GENERAL SECTION, MATERIAL=M1, ELSET=SS1M1,
ORIENTATION=COR1

0.0

,

*END PART

**===

APPENDIX B

PERMISSIONS FOR REPRINTS

1. Permission for figure 2.1 and 2.2

Bharath Koya <bk63@zips.uakron.edu> Oct 14

to Bartlebycom

Dear Sir,

I am Bharath Koya, graduate student from the Department of Biomedical Engineering, University of Akron. As part of my master's thesis, I have done work on the computational modeling of medial patellofemoral ligament reconstruction.

I have found pictures of the knee. I wish to reuse it in my thesis documentation.

I would be highly obliged and grateful if you could kindly grant me the permission to do so.

--

- Thanking You,

Kind Regards,

Bharath Koya.

Graduate Student,

Department of Biomedical Engineering,

The University of Akron,

Akron, Ohio.

Bartlebycom

to me

Thanks for your note.

Please consider this email permission to use the material listed in the manner described.

See the bibliographic record for this work for citation information.

Sincerely,

Steven van Leeuwen

President, Bartleby.com, Inc.

2. Perrmission for figure 2.3

3. Permission for figure 2.4

PERMISSION LICENSE AGREEMENT

P4971.JBJSInc.JBJS Am.Kaufer.1882.University of Akron.Koya

JBJSInc.JBJS Am.Kaufer.1882

10/17/2013

INVOICE ATTACHED

Dr. Bharath Koya

University of Akron
195 Wheeler St, Apt 205
Akron, Ohio 44304

Dear Dr. Koya,

Thank you for your interest in JBJS [Am] material. Please note: This permission does not apply to any figure or other material that is credited to any source other than JBJS. It is your responsibility to validate that the material is in fact owned by JBJS. If material within JBJS material is credited to another source (in a figure legend, for example) then any permission extended by JBJS is invalid. We encourage you to view the actual material at www.ejbjs.org or a library or other source. Information provided by third parties as to credits that may or may not be associated with the material may be unreliable.

We are pleased to grant you non-exclusive, nontransferable permission, limited to the format described below, and provided you meet the criteria below. Such permission is for one-time use and does not include permission for future editions, revisions, additional printings, updates, ancillaries, customized forms, any electronic forms, Braille editions, translations or promotional pieces unless otherwise specified below. We must be contacted for permission each time such use is planned. This permission does not include the right to modify the material. Use of the material must not imply any endorsement by the copyright owner. This permission is not valid for the use of JBJS logos or other collateral material, and may not be resold.

Abstracts or collections of abstracts and all translations must be approved by publisher's agent in advance, and in the case of translations, before printing. No financial liability for the project will devolve upon JBJS, Inc. or on Rockwater, Inc.. All expenses for translation, validation of translation accuracy, publication costs and reproduction costs are the sole responsibility of the foreign language sponsor. The new work must be reprinted and delivered as a stand-alone piece and may not be integrated or bound with other material. JBJS does not supply photos or artwork; these may be downloaded from the JBJS website, scanned, or (if available) obtained from the author of the article.

PERMISSION IS VALID FOR THE FOLLOWING MATERIAL ONLY:
2A and 2B
Journal of Bone and Joint Surgery Amercian, December, 1971, 53, 8, Mechanical Function of Patella, Kaufer, 1551-1560
IN THE FOLLOWING WORK ONLY:
electronic and/or print copies of figures in Master's thesis, University of Akron, no commercial use
CREDIT LINE(S) must be published next to any figure, and/or if permission is granted for electronic form, visible at the same time as the content republished with a hyperlink to the publisher's home page.

WITH PAYMENT OF PERMISSIONS FEE. License, once paid, is good for one year from your anticipated publication date unless otherwise specified above. Failure to pay the fee(s) or to follow instructions here upon use of the work as described here, will result in automatic termination of the license or permission granted. All information is required. Payment should be made to Rockwater, Inc. by check or credit card, via mail

Please contact Beth Ann Rocheleau at jbjs@rockwaterinc.com or 1-803-359-4578 with questions.

INVOICE 4971

10/17/2013

University of Akron
195 Wheeler St, Apt 205
Akron, Ohio 44304

payable to:

Rockwater, Inc.
Attn: Permissions JBJS
PO Box 2211
Lexington, SC 29071 USA
Federal Tax ID # 20-2561394

US Dollars ONLY by check or credit card. Please submit payment ONLY mail. Please do not email credit card information; it is not secure. Rockwater is not responsible for the security of emailed credit card information. The party purchasing permission is responsible for payment of tax as may be required by law.

permission fee: fee waived

Card Number	
American Express ☐ MasterCard ☐ Visa ☐	
Expiration date	**Security Code (3 or 4 digit)**
FIRST name (as shown on card)	**LAST name (as shown on card)**
COMPLETE Billing Address (associated with this card)	
Billing street address	
Billing City	
Billing County	
Billing State or Province	
Billing Country	
Billing Postal Code	
Cardholder telephone	
Cardholder signature	

Submission of form conveys acceptance of terms and conditions stated here.
Limitation of Liability and Disclaimer of Warranty: Rockwater, Inc. and Journal of Bone and Joint Surgery, Inc. and Journal of Bone and Joint Surgery, American edition (JBJS Am) make no warrantees with respect to the material presented here or the material for which permission is being granted; do not assume any expressly disclaim and liability for any loss or damage caused be errors or omissions whether such error or omissions result from negligence, accident or otherwise; and specifically disclaim any warranty of quality, performance, merchantability or fitness for a specific purpose. In no event will Rockwater, Inc. or JBJS, Inc., or JBJS Am be liable for any direct, indirect, special, incidental or consequential damages, including without limitation any lost profits, lost savings, lost revenues, loss of data, or costs of recovery, arising out of the use of or inability to use the material, regardless of whether such losses are foreseeable or whether such damages are deemed to result from the failure or inadequacy of any exclusive or other remedy.

4. Permission for figure 2.5

ELSEVIER LICENSE
TERMS AND CONDITIONS

Nov 04, 2013

This is a License Agreement between Bharath Koya ("You") and Elsevier ("Elsevier") provided by Copyright Clearance Center ("CCC"). The license consists of your order details, the terms and conditions provided by Elsevier, and the payment terms and conditions.

All payments must be made in full to CCC. For payment instructions, please see information listed at the bottom of this form.

Supplier	Elsevier Limited The Boulevard,Langford Lane Kidlington,Oxford,OX5 1GB,UK
Registered Company Number	1982084
Customer name	Bharath Koya
Customer address	195 Wheeler st AKRON, OH 44304
License number	3240970020270
License date	Oct 02, 2013
Licensed content publisher	Elsevier
Licensed content publication	The Knee
Licensed content title	Anatomy and biomechanics of the medial patellofemoral ligament
Licensed content author	A.A. Amis,P. Firer,J. Mountney,W. Senavongse,N.P. Thomas
Licensed content date	September 2003
Licensed content volume number	10
Licensed content issue number	3
Number of pages	6
Start Page	215
End Page	220
Type of Use	reuse in a thesis/dissertation
Portion	figures/tables/illustrations
Number of figures/tables/illustrations	1
Format	electronic

Are you the author of this Elsevier article?	No
Will you be translating?	No
Order reference number	None
Title of your thesis/dissertation	A FINITE ELEMENT STUDY ON MEDIAL PATELLOFEMORAL LIGAMENT RECONSTRUCTION
Expected completion date	Dec 2013
Estimated size (number of pages)	100
Elsevier VAT number	GB 494 6272 12
Permissions price	0.00 USD
VAT/Local Sales Tax	0.0 USD / 0.0 GBP
Total	**0.00 USD**
Terms and Conditions	

5. Permission for figure 2.6 and 2.7

PERMISSION LICENSE AGREEMENT

P4926.JBJSInc.JBJS Am.LaPrade.864.University of Akron.Koya

JBJSInc.JBJS Am.LaPrade.864

10/4/2013

Mr. Bharath Koya

INVOICE ATTACHED

University of Akron

,

Dear Mr. Koya,

Thank you for your interest in JBJS [Am] material. Please note: This permission does not apply to any figure or other material that is credited to any source other than JBJS. It is your responsibility to validate that the material is in fact owned by JBJS. If material within JBJS material is credited to another source (in a figure legend, for example) then any permission extended by JBJS is invalid. We encourage you to view the actual material at www.ejbjs.org or a library or other source. Information provided by third parties as to credits that may or may not be associated with the material may be unreliable.

We are pleased to grant you non-exclusive, nontransferable permission, limited to the format described below, and provided you meet the criteria below. Such permission is for one-time use and does not include permission for future editions, revisions, additional printings, updates, ancillaries, customized forms, any electronic forms, Braille editions, translations or promotional pieces unless otherwise specified below. We must be contacted for permission each time such use is planned. This permission does not include the right to modify the material. Use of the material must not imply any endorsement by the copyright owner. This permission is not valid for the use of JBJS logos or other collateral material, and may not be resold.

Abstracts or collections of abstracts and all translations must be approved by publisher's agent in advance, and in the case of translations, before printing. No financial liability for the project will devolve upon JBJS, Inc. or on Rockwater, Inc.. All expenses for translation, validation of translation accuracy, publication costs and reproduction costs are the sole responsibility of the foreign language sponsor. The new work must be reprinted and delivered as a stand-alone piece and may not be integrated or bound with other material. JBJS does not supply photos or artwork; these may be downloaded from the JBJS website, scanned, or (if available) obtained from the author of the article.

PERMISSION IS VALID FOR THE FOLLOWING MATERIAL ONLY:
Figures 2 and 3
Journal of Bone and Joint Surgery Amercian, September, 2007, 89, 9, The Anatomy of the Medial Part of the Knee, LaPrade, 2000-2010
IN THE FOLLOWING WORK ONLY:
electronic and/or print copies of academic thesis: "A Finite Element Study on Medial Patellofemoral Ligament Reconstruction" University of Akron, no commercial use
CREDIT LINE(S) must be published next to any figure, and/or if permission is granted for electronic form, visible at the same time as the content republished with a hyperlink to the publisher's home page.

WITH PAYMENT OF PERMISSIONS FEE. License, once paid, is good for one year from your anticipated publication date unless otherwise specified above. Failure to pay the fee(s) or to follow instructions here upon use of the work as described here, will result in automatic termination of the license or permission granted. All information is required. Payment should be made to Rockwater, Inc. by check or credit card, via mail

Please contact Beth Ann Rocheleau at jbjs@rockwaterinc.com or 1-803-359-4578 with questions.

INVOICE 4926 10/4/2013

University of Akron

,

payable to:

Rockwater, Inc.
Attn: Permissions JBJS
PO Box 2211
Lexington, SC 29071 USA
Federal Tax ID # 20-2561394

US Dollars ONLY by check or credit card. Please submit payment ONLY mail. Please do not email credit card information; it is not secure. Rockwater is not responsible for the security of emailed credit card information. The party purchasing permission is responsible for payment of tax as may be required by law.

permission fee: **fee waived, no commercial use**

Card Number	
American Express ☐ MasterCard ☐ Visa ☐	
Expiration date	**Security Code (3 or 4 digit)**
FIRST name (as shown on card)	**LAST name (as shown on card)**
COMPLETE Billing Address (associated with this card)	
Billing street address	
Billing City	
Billing County	
Billing State or Province	
Billing Country	
Billing Postal Code	
Cardholder telephone	
Cardholder signature	

Submission of form conveys acceptance of terms and conditions stated here.
Limitation of Liability and Disclaimer of Warranty: Rockwater, Inc. and Journal of Bone and Joint Surgery, Inc. and Journal of Bone and Joint Surgery, American edition (JBJS Am) make no warrantees with respect to the material presented here or the material for which permission is being granted; do not assume any expressly disclaim and liability for any loss or damage caused be errors or omissions whether such error or omissions result from negligence, accident or otherwise; and specifically disclaim any warranty of quality, performance, merchantability or fitness for a specific purpose. In no event will Rockwater, Inc. or JBJS, Inc., or JBJS Am be liable for any direct, indirect, special, incidental or consequential damages, including without limitation any lost profits, lost savings, lost revenues, loss of data, or costs of recovery, arising out of the use of or inability to use the material, regardless of whether such losses are foreseeable or whether such damages are deemed to result from the failure or inadequacy of any exclusive or other remedy.

6. Permission for figure 2.8

License Details

This is a License Agreement between Bharath Koya ("You") and Elsevier ("Elsevier"). The license consists of your order details, the terms and conditions provided by Elsevier, and the payment terms and conditions.

Get the printable license.

License Number	3262000312881
License date	Nov 04, 2013
Licensed content publisher	Elsevier
Licensed content publication	Arthroscopy: The Journal of Arthroscopic & Related Surgery
Licensed content title	Reconstruction of the Medial Patellofemoral Ligament With Autologous Quadriceps Tendon
Licensed content author	Frank R. Noyes,Jay C. Albright
Licensed content date	August 2006
Licensed content volume number	22
Licensed content issue number	8
Number of pages	7
Type of Use	reuse in a thesis/dissertation
Portion	figures/tables/illustrations
Number of figures/tables/illustrations	1
Format	electronic
Are you the author of this Elsevier article?	No
Will you be translating?	No
Order reference number	None
Title of your thesis/dissertation	A FINITE ELEMENT STUDY ON MEDIAL PATELLOFEMORAL LIGAMENT RECONSTRUCTION
Expected completion date	Dec 2013
Estimated size (number of pages)	100
Elsevier VAT number	GB 494 6272 12
Permissions price	0.00 USD
VAT/Local Sales Tax	0.00 USD / 0.00 GBP
Total	**0.00 USD**

7. Permission for figure 2.9

License Details

This is a License Agreement between Bharath Koya ("You") and Elsevier ("Elsevier"). The license consists of your order details, the terms and conditions provided by Elsevier, and the payment terms and conditions.

Get the printable license.

License Number	3246350499669
License date	Oct 12, 2013
Licensed content publisher	Elsevier
Licensed content publication	Orthopaedics and Trauma
Licensed content title	(vii) Patellofemoral instability
Licensed content author	Neil Upadhyay,Charles Wakeley,Jonathan D.J. Eldridge
Licensed content date	April 2010
Licensed content volume number	24
Licensed content issue number	2
Number of pages	10
Type of Use	reuse in a thesis/dissertation
Portion	figures/tables/illustrations
Number of figures/tables/illustrations	10
Format	electronic
Are you the author of this Elsevier article?	No
Will you be translating?	No
Order reference number	None
Title of your thesis/dissertation	A FINITE ELEMENT STUDY ON MEDIAL PATELLOFEMORAL LIGAMENT RECONSTRUCTION
Expected completion date	Dec 2013
Estimated size (number of pages)	100
Elsevier VAT number	GB 494 6272 12
Permissions price	0.00 USD
VAT/Local Sales Tax	0.00 USD / 0.00 GBP
Total	**0.00 USD**

8. Permission for figure 2.11

License Details

This is a License Agreement between Bharath Koya ("You") and Elsevier ("Elsevier"). The license consists of your order details, the terms and conditions provided by Elsevier, and the payment terms and conditions.

Get the printable license.

License Number	3240941301897
License date	Oct 02, 2013
Licensed content publisher	Elsevier
Licensed content publication	Clinical Biomechanics
Licensed content title	Hamstrings loading contributes to lateral patellofemoral malalignment and elevated cartilage pressures: An in vitro study
Licensed content author	John J. Elias,Marcus S. Kirkpatrick,Archana Saranathan,Saandeep Mani,Laura G. Smith,Miho J. Tanaka
Licensed content date	October 2011
Licensed content volume number	26
Licensed content issue number	8
Number of pages	6
Type of Use	reuse in a thesis/dissertation
Portion	figures/tables/illustrations
Number of figures/tables/illustrations	1
Format	electronic
Are you the author of this Elsevier article?	No
Will you be translating?	No
Order reference number	None
Title of your thesis/dissertation	A FINITE ELEMENT STUDY ON MEDIAL PATELLOFEMORAL LIGAMENT RECONSTRUCTION
Expected completion date	Dec 2013
Estimated size (number of pages)	100
Elsevier VAT number	GB 494 6272 12
Permissions price	0.00 USD
VAT/Local Sales Tax	0.00 USD / 0.00 GBP
Total	**0.00 USD**

9. Permission for figure 2.12

WOLTERS KLUWER HEALTH LICENSE TERMS AND CONDITIONS

Nov 04, 2013

This is a License Agreement between Bharath Koya ("You") and Wolters Kluwer Health ("Wolters Kluwer Health") provided by Copyright Clearance Center ("CCC"). The license consists of your order details, the terms and conditions provided by Wolters Kluwer Health, and the payment terms and conditions.

All payments must be made in full to CCC. For payment instructions, please see information listed at the bottom of this form.

License Number	3240931439853
License date	Oct 02, 2013
Licensed content publisher	Wolters Kluwer Health
Licensed content publication	Medicine & Science in Sports & Exercise
Licensed content title	Dual Fluoroscopic Analysis of the Posterior Cruciate Ligament-Deficient Patellofemoral Joint during Lunge.
Licensed content author	VAN DE VELDE, SAMUEL; GILL, THOMAS; LI, GUOAN
Licensed content date	Jan 1, 2009
Volume Number	41
Issue Number	6
Type of Use	Dissertation/Thesis
Requestor type	Individual Account
Author of this Wolters Kluwer article	No
Title of your thesis / dissertation	A FINITE ELEMENT STUDY ON MEDIAL PATELLOFEMORAL LIGAMENT RECONSTRUCTION
Expected completion date	Dec 2013
Estimated size(pages)	100
Billing Type	Invoice
Billing address	195 Wheeler st Apt 205 AKRON, OH 44304 United States
Total	**0.00 USD**